EPOXY LAYERED SILICATE NANOCOMPOSITES AS MATRIX IN FIBRE REINFORCED COMPOSITES

A

Thesis Report

Submitted in partial fulfillment of the requirement for the award of degree

MASTER OF ENGINEERING

in

CAD/CAM & ROBOTICS

Submitted By

SUMIT MAHAJAN

(Roll No. 800981025)

Under Guidance of

Mr. BIKRAMJIT SHARMA
Assistant Professor
Deptt. of Mechanical Engg.
Thapar University, Patiala

Dr. RAJEEV MEHTA
Associate Professor
Deptt. of Chemical Engg.
Thapar University, Patiala

DEPARTMENT OF MECHANICAL ENGINEERING

THAPAR UNIVERSITY

PATIALA-147004, INDIA

CERTIFICATE

This is to certify that the work in this thesis report entitled "**Epoxy Layered Silicate Nanocomposites as Matrix in Fibre Reinforced Composites**" submitted in partial fulfillment of requirement for the award of **Master of Engineering Degree in CAD/CAM & Robotics** in Mechanical Engineering Department of Thapar University, Patiala, is an authentic record of work carried out by me under the guidance of **Mr. Bikramjit Sharma,** Assistant Professor, Mechanical Engineering Department, Thapar University, Patiala **and Dr. Rajeev Mehta,** Associate Professor, Chemical Engineering Department, Thapar University Patiala.

The matter embodied in this report has not been submitted in part or full to any university or institute for the award of any degree.

Sumit Mahajan

Dated: 15/07/2011 **Sumit Mahajan**

This is to certify that the above declaration made by the student concern is correct to the best of my knowledge and belief.

Mr. Bikramjit Sharma
Assistant Professor
Deptt. of Mechanical Engg.
Thapar University, Patiala

Rajeev Mehta

Dr. Rajeev Mehta
Associate Professor
Deptt. of Chemical Engg.
Thapar University, Patiala

Dr. Ajay Batish
Professor & Head
Deptt. of Mechanical Engg.
Thapar University, Patiala

Countersigned by:

S.K. Mohapatra
Dean Academic Affairs
Thapar University, Patiala

ACKNOWLEDGEMENT

I am highly grateful to the authorities of Thapar University, Patiala for providing this opportunity to carry out the research/Theses work.

I would like to express a deep sense of gratitude and thank profusely my thesis guide **Mr. Bikramjit Sharma**, Assistant Professor, Mechanical Engineering Department, Thapar University, Patiala and **Dr. Rajeev Mehta**, Associate Professor, Chemical Engineering Department, Thapar University, Patiala for their sincere & invaluable guidance, suggestions and attitude which inspired me to submit report in the present form.

I am highly thankful to **Dr. Rahul Chibber**, Assistant professor, Mechanical Engineering Department and **Mr. Ranpreet Singh** (Ph.D Scholar in Chemical Engineering Department) for his invaluable guidance & continuous support.

I heartily thank to **Mr. Purshottam Kumar Singh** and **Mr. Ravi Shukla** for helping me in conducting the tests on S.E.M. machine and XRD machine.

I am also thankful to other faculty members and all the workshop staff of Mechanical Department, Thapar University, Patiala for their support.

I would also like to thank and acknowledge **BASF Construction Chemicals (India) Private Limited and Connell Bros. Mumbai** for supplying us generously with E-Glass Fibre sheet, M Brace epoxy (Base and hardener) and Clay (Closite 30B) etc. for this experimentation.

My special thanks are due to my family members and friends who constantly encouraged me to complete this study.

Sumit Mahajan

ABSTRACT

An economical and viable option to conventional and high cost materials is the use of fiber glass/epoxy composites, but for impact applications their toughness still has to be enhanced. The toughness and other mechanical properties can be improved by using very small amount of nanoclay into an epoxy system. In the present work epoxy modified with Closite 30B (1 wt%, 3 wt% and 5 wt%) nanoclay is used with E-glass unidirectional fibers to manufacture fiber reinforced nanocomposite using hand layup method. The nanocomposites have been characterized using XRD and SEM. The mechanical properties are measured by carrying out tensile tests, hardness tests and flexural tests, values are compared with those found for fiber reinforced epoxy composites. The mechanical test shows that the presence of 3 wt% nano-clay largely increases tensile and flexural strength. The flexural and tensile properties have to be improved by 57% and 8% respectively by adding 3 wt% of nanoclay. Micro hardness improved at 3 wt% of nanoclay loading and then decreased at further loading. Further durability studies on nanocomposites have been performed in water and NaOH baths under accelerated hygrothermal loading. Water uptake of epoxy was reduced by the addition of glass fiber and nanoclay. During exposure it is observed that the properties degradation in NaOH environment was more severe as compared to simple water.

TABLE OF CONTENTS

LIST OF FIGURES

LIST OF TABLES

NOMENCLATURE AND ABBREVIATIONS

S.No.	Nomenclature	Abbreviations
1.	**GFRP**	Glass fiber reinforced composites
2.	**VLSI**	Very large scale integration
3.	**PNC**	Polymer nanocomposites
4.	**OMMT**	Monomorillonite organoclay
5.	**CNF's**	Carbon nanofibres
6.	**CNT's**	Carbon nanotubes
7.	**WXRD**	Wide angle x-ray diffraction
8.	**PAN**	Polyacrylonitrile
9.	**SEM**	Scanning electron microscope
10.	**CTE**	Coefficient of thermal expansion
11.	**VGCF**	Vapor grown carbon fiber
12.	**DSC**	Differential scanning calorimeter
13.	**CAI**	Compression after impact
14.	**NFG**	Natural graphite flakes

CHAPTER 1 INTRODUCTION

Nanotechnology involves the control and manipulation of materials at the nanoscale (particle sizes from 1 to 100 nanometre (nm)), where 1 nm equals 1 billionth of a meter) to create new materials and structures that have novel properties due to their small size (increased surface area) is a topic of great current research [Jena ed, 1996]. Materials with feature on the scale nanometres (10^{-9}meter) often have properties dramatically different from their bulk-scale counterparts [Sakaki, 1994]. At nanolevel, some compounds transform from inert to active, from electrical insulator to conductors, from fragile to tough. They can become stronger, lighter and more resistant. These transformed properties are what account for the infinite potential application of nanoparticles. One of the major factors, which alter these properties, is the increase in the ratio of surface area to volume. As the surface area of a particle increases exponentially, creating more sites for bonding, catalysis or reaction with surroundings material, resulting in improved properties such as increased strength or chemical or heat resistance. Hence, due to the high surface-to volume ratio associated with nanometre sized particles it is possible to control the fundamental properties of materials through the surface/size effect. There is a great variety of nanomaterials and their range of properties and possible applications appears to be enormous, from extra-ordinary tiny electronics devices, including miniature batteries, to biomedical uses and as components of parts of automobiles. In addition to this, in the field of VLSI, nanocomposites can be used as electromagnetic shielding between interconnects. Additionally the fact that nanoparticles have dimensions below the visible wavelength of light, i.e. cannot scatter light, that's why the resulting nanoproduct is transparent, and which has other implications also.

Nanotechnology is directed towards the formation of various nanomaterials such as:

- Nanocomposites
- Nanofiber
- Nanoparticulate fillers
- Nanoporous

1.1 Composite

Composite materials are engineered materials made from two or more constituent materials with significantly different physical or chemical properties which remain separate and distinct on a macroscopic level within the finished structure. Composites are made up of individual materials referred to as constituent materials.

There are two categories of constituent materials: matrix and reinforcement. At least one portion of each type is required. The matrix material surrounds and supports the reinforcement materials by maintaining their relative positions. The reinforcements impart their special mechanical and physical properties to enhance the matrix properties.

1.1.1 Composites have two phases:

- **Matrix phase**

  The primary phase, having a continuous character, is called matrix. Matrix is usually more ductile and less hard phase. It holds the dispersed phase and shares a load with it.

- **Dispersed (reinforcing) phase**

  The second phase (or phases) is imbedded in the matrix in a discontinuous form. This secondary phase is called dispersed phase. Dispersed phase is usually stronger than the matrix, therefore it is sometimes called reinforcing phase.

1.1.2 Properties of composites depend on

- properties of phases
- geometry of dispersed phase (particle size, distribution, orientation)
- amount of phase

1.2 Classification of Composite

Composites can be broadly classified in to two groups as shown in Fig. 1.1.

1.2.1 Natural Composites: Several natural materials can be grouped under natural composites, e.g. Bones, wood, shells, pearlite (steel which is a mixture of a phase and Fe_3C) etc.

1.2.2 Man-Made Composites: Man-made composites are produced by combining two or more materials in definite proportions under controlled conditions. e.g. Mud mixed straw to produce

stronger mud mortar and bricks, Plywood, Chipboards, Decorative laminates, Fiber Reinforced Plastic (FRP), Carbon Composites, Concrete and RCC, Reinforced Glass etc

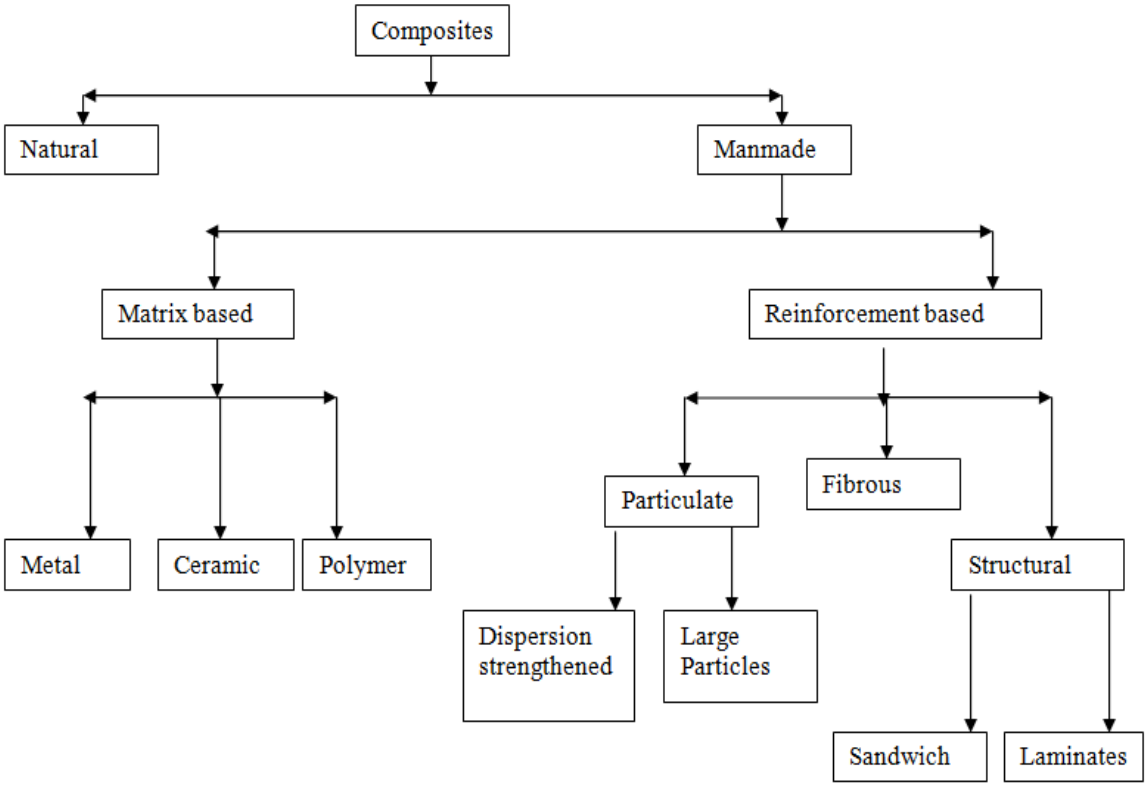

Fig. 1.1 Classification of composite materials

1.3 Uses of Composite Materials

- Extensively used in space technology and production of Aerospace Components (tails, wings etc.)
- Used in the production of sport goods e.g. racing car bodies and bicycle frames etc.
- Used for general industrial and engineering structures
- Used in high speed and fuel efficient transport vehicles
- Carbon composite is a key material in today's launch vehicles and spacecraft. It is widely used in solar panel substrates, antenna reflectors and yokes of spacecraft. It is also used in payload adapters, inter-stage structures and heat shields of launch vehicles.

1.4 Introduction to Fibre Reinforced Polymers (FRP)

Fiber-reinforced polymer (**FRP**) is a composite material made of a polymer matrix reinforced with fibers. The fibers are usually fiberglass, carbon or aramid, while the polymer is usually an epoxy, vinyl ester or polyester thermosetting plastic. FRPs are commonly used in the aerospace, automotive, marine, and construction industries. The strength properties of FRP collectively make up one of the primary reasons for which civil engineers select them in the design of structures. A material's strength is governed by its ability to sustain a load without excessive deformation or failure. When an FRP specimen is tested in axial tension, the applied force per unit cross-sectional area (stress) is proportional to the ratio of change in a specimen's length to its original length (strain). When the applied load is removed, FRP returns to its original shape or length. In other words, FRP responds linear-elastically to axial stress. The response of FRP to axial compression is reliant on the relative proportion in volume of fibres, the properties of the fibre and resin, and the interface bond strength. FRP's response to transverse tensile stress is very much dependent on the properties of the fiber and matrix, the interaction between the fiber and matrix, and the strength of the fiber-matrix interface. Generally tensile strength in this direction is very poor.

1.5 Advantages of Fibre Reinforced Polymers:

1. High strength to weight ratio
2. Corrosion resistant
3. Can be tailored for the application (both shape and type of FRP)
4. FRP has a low cost considering other materials
5. Cost of installation versus replacement is low
6. Cost of installation time (both direct and indirect) is also low.

1.6 Nanocomposites

A nano-composite is as a multiphase solid material where one of the phases has one, two or three dimensions of less than 100 nanometer (nm), or structures having nano-scale repeat distances between the different phases that make up the material. In the broadest sense this definition can include porous media, colloids, gels and copolymer, but is more usually taken to mean the solid combination of a bulk matrix and nano-dimensional phase(s) differing in properties due to

dissimilarities in structure and chemistry. The mechanical, electrical, thermal, optical, electrochemical, catalytic properties of the nano-composite will differ markedly from that of the component materials. Size limits for these effects have been proposed, <5 nm for catalytic activity, <20 nm for making a hard magnetic material soft, <50 nm for refractive index changes, and <100 nm for achieving superparamagnetism, mechanical strengthening or restricting matrix dislocation movement.

Nanocomposites are found in nature, for example in the structure of the abalone shell and bone. The use of nanoparticle-rich materials long predates the understanding of the physical and chemical nature of these materials. Jose-Yacaman *et al.* (1996) investigated the origin of the depth of color and the resistance to acids and bio-corrosion of maya blue paint, attributing it to a nanoparticle mechanism. From the mid 1950s nanoscale organo-clays have been used to control flow of polymer solutions (e.g. as paint viscosifiers) or the constitution of gels (e.g. as a thickening substance in cosmetics, keeping the preparations in homogeneous form). By the 1970s polymer/nano composites were the topic of textbooks, although the term "nanocomposites" was not in common use.

In mechanical terms, nanocomposites differ from conventional composites due to the exceptionally high surface to volume ratio of the reinforcing phase and/or its exceptionally high aspect ratio. The reinforcing material can be made up of particles (e.g. minerals), sheets (e.g. exfoliated clay stacks) or fibers (e.g. carbon nanotubes or electro spun fibers). The area of the interface between the matrix and reinforcement phase(s) is typically an order of magnitude greater than for conventional composite materials. The matrix material properties are significantly affected in the vicinity of the reinforcement. Ajayan *et al.* (1992) note that with polymer nanocomposites, properties related to local chemistry, degree of thermo set cure, polymer chain mobility, polymer chain conformation, degree of polymer chain ordering or crystallinity can all vary significantly and continuously from the interface with the reinforcement into the bulk of the matrix.

This large amount of reinforcement surface area means that a relatively small amount of nanoscale reinforcement can have an observable effect on the macro scale properties of the composite. For example, adding carbon nanotubes improves the electrical and thermal conductivity. Other kinds of nanoparticulates may result in enhanced optical properties, dielectric properties, heat resistance or mechanical properties such as

stiffness, strength and resistance to wear and damage. In general, the nano reinforcement is dispersed into the matrix during processing. The percentage by weight (called *mass fraction*) of the nanoparticulates introduced can remain very low (on the order of 0.5% to 5%) due to the low filler pre-location, threshold especially for the most commonly used non-spherical, high aspect ratio fillers (e.g. nanometer-thin platelets, such as clays, or nanometer-diameter cylinders, such as carbon nanotubes).

1.7 Polymer Nanocomposites

For many fields of the modern industry appreciable improvement of physicomechanical properties of polymeric materials is desirable. Nowadays, the most perspective decision of this problem is a modification polymer with nanostructure modifiers – creation of polymeric nanocomposites. Polymer nanocomposites (PNC) are polymers (thermoplastics, thermo sets, elastomers) that have been reinforced with small quantities (less than 5% by weight) of nano-sized particles. Molecular interaction between polymer and nanofillers do not posses. Uniform dispersion of nanoparticles in polymer matrix produces ultra- large interfacial area per volume between the nanoparticle and the host polymer. This immense internal interfacial area and the nanoscopic dimension between nanopartical fundamentally differentiate PNCs from traditional composites and filled plastics. Introduction to nanoparticles to polymer matrix ensure significant property improvements with very low loading levels. Traditional micro particles additives require much higher filler concentration to achieve similar results. The most commonly used nano fillers are:

1. Manomorillonite organoclays (MMT)
2. Carbon Nanofiber (CNFs)
3. Carbon nanotubes (CNTs)
4. Metallic nanoparticles
5. Others

The value of PNC technology comes from providing value added properties not present in the neat polymer, without sacrificing the inherent processibility and mechanical properties of the polymer. Some of the major advantages of the polymer nanocomposites are:

Mechanical properties:

- High adhesion of nanoparticles to polymer matrix result in the enhanced strength of nanocomposites relative to conventional composite.
- Small size of nanoparticles ensures small size of pores in the case of exfoliation of a matrix from filler particles. It results in the strength increase too.
- Introduction of small amount of nanoparticles to polymer significantly enhance the adhesion of polymer to different substance.

Optical properties:

- Nanocomposites are optically more transparent in comparison to conventional composites.
- Special optical effects.
- Optical clarity in comparison to conventionally filled polymers.

Magnetic properties:

- In some case composites with magnetic nanoparticles have the magneto resistance and magnetic permeability much higher than in the case of conventional composites.
- It is possible to make composites with magnetic threshold concentration smaller than electrical percolation threshold.

1.8 Epoxy Nanocomposites

In 1946, the first industrially-produced epoxy resin was introduced to market. Since then, the use of thermosetting polymers has steadily increased. The wide range of epoxy resin applications includes: coating, electrical, automotive, marine, aerospace and civil infrastructure as well as tool fabrication and pipes and vessels in the chemical industry. Due to their low density of around 1.3 g/cm and good adhesive and mechanical properties, epoxy resin became a promising material for high performance applications in the transport industry, usually in the form of composite materials such as fiber composite or in honeycomb structures. In the aerospace industry, epoxy-composites material can be found in various part of the body and structure of military and civil aircrafts, with the number of applications on the rise. A recent approach to improve and diversify polymer properties in the aerospace industries is through the dispersion of nanometer-scaled fillers in the polymer matrix. [Njuguna and Pielichowski, 2003]. A significant number of academic and industrial projects have investigated the possibilities to further improve epoxy

resin (and in some cases composites or other binary systems) through the strategy of producing nanocomposites.

The term ‘epoxy resin’ refers to both the polymer and its cured resin/hardener system. The former is a low molecular weight oligomer that contains one or more epoxy groups per molecule (more than one unit per molecule is required if the resultant material is to be cross-linked). The characteristic group, a three-member ring known as epoxy, epoxide, oxirane, glycidyl or ethoxyline group is highly strained and therefore very reactive. Epoxy resins can be cross-linked through a polymerization reaction with a hardener at room temperature or at elevated temperature (latent reaction). Curing agents are used for room temperature cure are usually aliphatic amines, whilst commonly used higher temperature, higher performance hardener are aromatic amines and acid anhydrides. However, an increasing number of specialized curing agents, such as poly-functional amines, polybasic carboxylic acids, mercaptans and inorganic hardener are also used. All of these results in different, tailored properties of the final polymer matrix. In general, the higher temperature Cured resin systems have improved properties, such as higher glass transition temperatures, strength and stiffness, compared to those cured at room temperature.

1.9 Clay Nanoparticales

Clay as nanoparticals such as smectic clays (e.g. montmorillonite) are incorporated into polymers to form resulting polymer nanocomposite, which may possess unique electrical, mechanical and optical properties. The presence of clay as filler is expected to strengthen the mechanical properties of PU even upon lower loading of filler. Fiber retardancy, barrier resistance and ion conductivity are also expected to be influenced by loading of clay as filler. As their name suggests, polymer/clay nanocomposites comprise organic/inorganic hybrid polymer matrices containing platelet-shaped clay particles that have sizes of the order of a few nanometers thick and several hundred nanometer long. Partly because of their aspect ratios and high surface areas, the clay particles, if properly dispersed in the polymer matrix at a loading level of 1 to 5 wt. %, impart unique combinations of physical and chemical properties that make these nanocomposites attractive for making films and coatings for a variety of industrial applications. Relative to the unmodified polymer, the polymer/clay nanocomposites may exhibit improvements in strength, modulus, and toughness, tear, radiation, fire resistance, and lower thermal expansion and

permeability to gases while retaining a high degree of optical transparency [www.techbriefs.com].

The most common type of nanoclay is montmorillonite (MMT), a layered aluminosilicate in the smectite family of clay. Unlike clay minerals such as talc and mica that have been used as fillers for years, MMT can be delaminated and dispersed into an individual layers only one nanometer thick by about 70 nm to 150 nm across. The result is a radical increase in the surface area-to-volume ratio: with a surface area of 750m^2/g, 20g of MMT platelets could cover a football field! Montmorillonite, can absorb 20-30 times its volume in water, and is of particular interest to the plastics industry. It is a 2:1 layered structured; a single layer of aluminum octahedra sandwiched between two layers of silicon tetrahedral. Each layered sheet is slightly less than one nanometer, with surface dimensions extending to about a micron (1,000 nanometers). With aspect ratios approaching 1,000, surface area of the clay is in the range of 750m^2/g.

According to the structure three different types of clay-polymer composites can be distinguished (Fig. 1.2) [Alexandre, 2000].

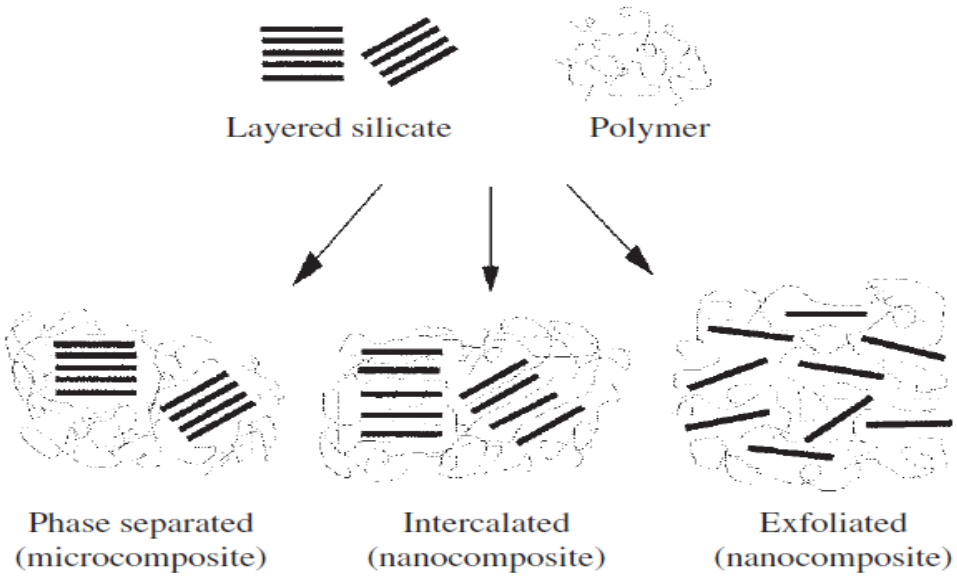

Fig. 1.2 Three idealized structures of polymer-clay composites

When the matrix polymer chains are unable to penetrate between the layers of the silicate particles a conventional composite is formed. Intercalated structures are formed when one or more polymer chains intercalate between the layers. Hereby the interlayer spacing is increased but the ordered layer structure of the clay particles is retained as can be observed by wide angle

X-ray diffraction (XRD). In exfoliated composites the clay particles are completely delaminated and the silicate layers do not show any periodicity in their arrangement.

Dispersing clay in the polymer is very difficult and therefore a compatibilizing agent is commonly used. Compatibilizing agent is a molecule constituted of one hydrophilic and one organophilic function. The compatibilizing agents allow dispersing layered silicates in polymers by substitutions of the metallic cat ions between the silicate layers.

1.10 Types of Fibre

A. Carbon Fibre

Carbon fibres are created when polyacrylonitrile fibres (PAN), Pitch resins, or Rayon are carbonized (through oxidation and thermal pyrolysis) at high temperatures. Through further processes of graphitizing or stretching the fibres strength or elasticity can be enhance respectively. Carbon fibres are manufactured in diameters analogous to glass fibres with diameters ranging from 9 to 17 μm. These fibres wound into larger threads for transportation and further production processes. Further production processes include weaving or braiding into carbon fabrics, cloths and mats analogous to those described for glass that can then be used in actual reinforcement processes (Fig. 1.3(a)).

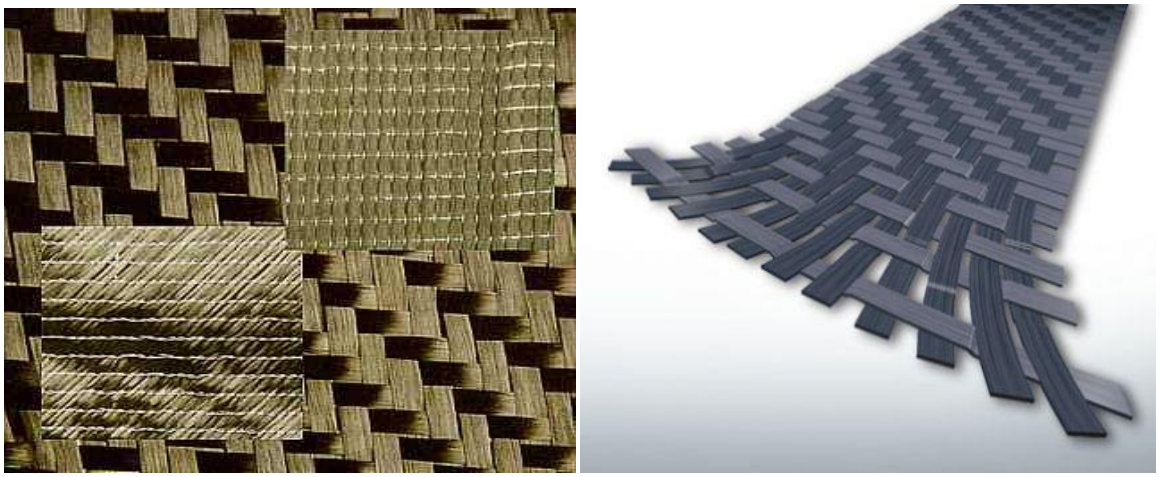

Fig. 1.3(a) Different types of matted carbon fibres

B. Glass Fibre

FRP plastics use textile glass fibers; textile fibers are different from other forms of glass fibers used for insulating applications. Textile glass fibers begin as varying combinations of SiO_2, Al_2O_3, B_2O_3, CaO, or MgO in powder form. These mixtures are then heated through a direct melt process to temperatures around 1300 degrees Celsius, after which dies are used to extrude filaments of glass fiber in diameter ranging from 9 to 17 µm. These filaments are then wound into larger threads and spun onto bobbins for transportation and further processing. Glass fiber is by far the most popular means to reinforce plastic and thus enjoys a wealth of production processes, some of which are applicable to aramid and carbon fibers as well owing to their shared fibrous qualities. Different types of glass fibre are shown in the Fig. 1.11(b).

Fig. 1.3(b) commercially available glass fibres

The types of glasses used for structural reinforcements are as follows:

1) **E-glass** (electrical) - lower alkali content and stronger than A glass (alkali). Good tensile and compressive strength and stiffness, good electrical properties and relatively low cost, but impact resistance relatively poor. E-glass is the most common form of reinforcing fibre used in polymer matrix composites.

2) **C-glass** (chemical) - best resistance to chemical attack. Mainly used in the form of surface tissue in the outer layer of laminates used in chemical and water pipes and tanks.

3) **R, S or T-glass** – manufacturers' trade names for equivalent fibres having higher tensile strength and modulus than E glass, with better wet strength retention. Higher ILSS and wet out properties are achieved through smaller filament diameter. Developed for aerospace and defense

industries, and used in some hard ballistic arm our applications. This factor, and low production volumes mean relatively high price.

Glass fibre is available in the following forms:

A. Continuous Fibre
B. Chopped strands
C. Woven Fabric.

1.11 Properties of Different Fibres

Materials	Density (g/cm^3)	Tensile Strength (MPa)	Young Modulus (GPa)
E-Glass	2.55	2000	80
S-Glass	2.49	4750	89
Alumina (Saffil)	3.28	1950	297
Carbon	2.00	2900	525
Kevlar 29	1.44	2860	64
Kevlar 49	1.44	3750	136

Fig. 1.4 Comparison of typical properties for some common fibre

1.12 Applications of Glass Fibre Reinforced Polymers

- Sailplanes, sports cars, karts, body shells, boats, kayaks, flat roofs, Lorries, wind turbine blades.
- Pods, domes and architectural features where a light weight is necessary.
- Bodies for automobiles.
- FRP tanks and vessels: FRP is used extensively to manufacture chemical equipments and tanks and vessels.
- UHF-broadcasting antennas are often mounted inside a glass-reinforced plastic cylinder on the pinnacle of a broadcasting tower.
- Engine intake manifolds are made from glass fiber reinforced PA 66.
- Automotive gas and clutch pedals made from glass fiber reinforced PA 66 (DWP 12-13)

1.13 Environmental effects on Fibre Composites

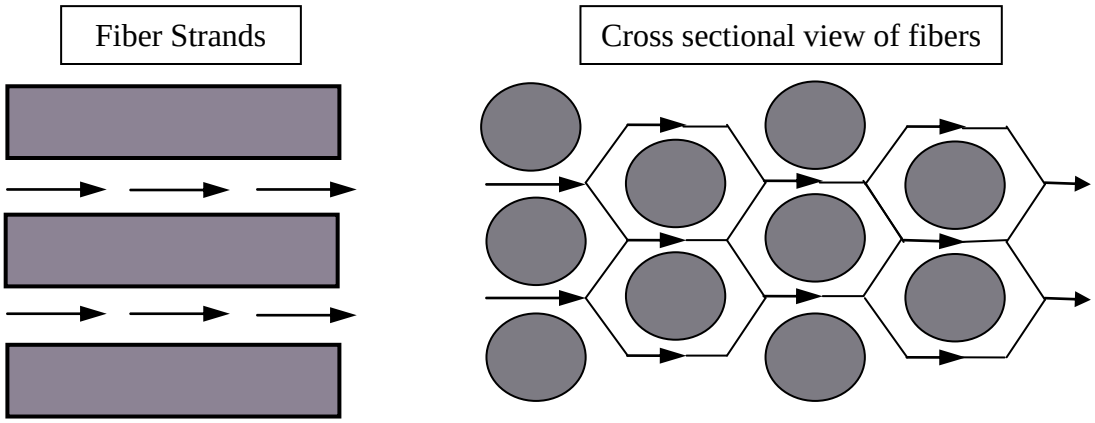

Fig. 1.5 Diffusion path of moisture into composite thickness direction

Fibrous composites, especially carbon fibre reinforced epoxy are increasingly being used in military and aerospace applications owing to several desirable properties including high specific strength, high specific stiffness and controlled anisotropy. Despite these advantages over conventional structural materials such as metals, composites are susceptible to heat and moisture when operating in harsh and changing environmental conditions. When exposed to humid environments, carbon–epoxy composites absorb moisture (Fig. 1.4) and undergo dilatational expansion.

The presence of moisture and the stresses associated with moisture induced expansion can result in lowered damage tolerance, with an adverse effect on long-term structural durability. The amount of moisture absorbed by the epoxy matrix is significantly greater than that by the carbon fibres, which absorb very little or no moisture. This result in a significant mismatch in the moisture induced volumetric expansion between the matrix and the fibres, and thus leads to the evolution of localized stress and strain fields in the composite.

Additionally, moisture absorption leads to changes in the thermo physical, mechanical and chemical characteristics of the epoxy matrix by plasticization and hydrolysis. These changes in the polymer structure lower both the elastic modulus and the glass transition temperature. At the same time, moisture wicking along the fibre matrix interface degrades the fibre matrix bond, resulting in loss of micro structural integrity. The net effect of moisture absorption is the deterioration of matrix-dominated properties such as compressive strength, interlaminar shear strength, fatigue resistance and impact tolerance .These factors lead to reduced damage tolerance and lack of long-term durability.

In homogeneous materials, the kinetics of moisture diffusion is governed by the maximum moisture content and the diffusivity. The maximum moisture content is defined by the net amount of moisture that a fully saturated material contains under steady state equilibrium when exposed to a given environmental condition. It is usually expressed as the ratio of the increase in weight per unit dry weight at the point of saturation. The relative weight gain approaches the maximum moisture content of composite at infinite time. It has been shown that the maximum moisture content strongly depends on the relative humidity of the exposure environment. Usually the maximum moisture content is determined by exposing the material to a humid environment for a long duration of time until steady state equilibrium is attained. This process often takes several months, which makes the procedure cumbersome and time consuming.

Also the rate of moisture diffusion is governed by the diffusivity. In general, the diffusivity is a strong function of the ambient temperature and a weak function of the relative humidity. In the case of composites, the diffusion process is more complex. It depends on the diffusivities of the individual constituents, their relative volume fractions, constituent arrangement and morphology. Traditionally, effective diffusivity has been used to predict the amount of moisture content. The figure 1.6 shows the various effects of moisture diffusion on a composite sample.

When a fibre-reinforced composite material is exposed to a hygrothermal environment and mechanical loads, changes in material properties are expected. These changes in material properties are connected to an irreversible material degradation. The moisture may affect the laminates through chemical changes such as relaxation and oxidation of the matrix material. A cyclic moisture environment exposed to a laminate may cause damage such as debonding at fibre/matrix interfaces and continuous cracks.

Usually one of the first observed damage modes in a laminated composite is *matrix cracking*. These cracks are in general not critical for final failure, but if they are connected to a surrounding moisture environment more rapid moisture absorption may be expected for the cracked laminate. The accelerated moisture absorption in a cracked material exposed to humid air is a result of the faster diffusion in air compared to the diffusion speed in the composite material. Faster moisture uptake may also develop a faster material degradation. This makes it important to know the moisture absorption behavior in a cracked laminate.

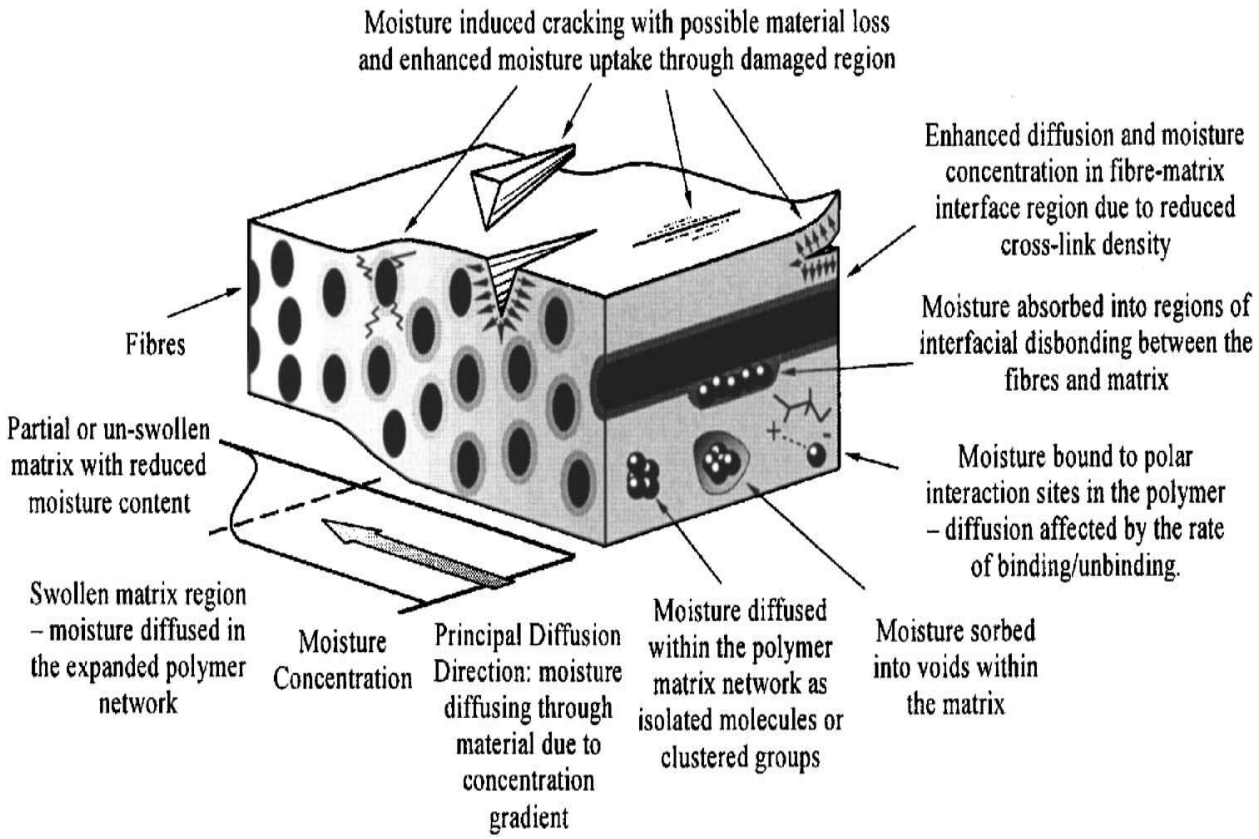

Fig. 1.6 Deteriorated fibre specimens under moist environmental condition

For an undamaged material, well-accepted moisture transportation models are available. The most common models for the transportation of moisture in undamaged polymeric composite materials are Fickian diffusion and Langmuir diffusion. If the material contains cracks that significantly affect the moisture uptake, then the original laws of Fickian and Langmuir are no longer valid for the whole laminate, but locally they still work. The influences of matrix cracks on moisture uptake in glass-fibre/epoxy laminates have been studied. Experiments, finite-element calculations and analytical calculations have been performed and the results are compared. The experimental results show that crack closure may occur early in the absorption process and that the crack closure is significantly influencing the moisture absorption.

CHAPTER 2 LITERATURE REVIEW

Extensive literature review has been carried out for defining the research problem. Most of the work carried out is on the characterization of composites made by adding nanofillers to matrix system. GFRP with nanoclay and their environmental degradation under different conditions has not been addressed so far.

Wang *et al.* (2001) were prepared polymeric nano-composites by melt intercalation. In this study, nano-clay was mixed with a polymer by twin-screw extrusion. The clay-spacing in the composites was measured by X-ray diffraction (XRD). The morphology of the composites and its development during the extrusion process were observed by scanning electron microscopy **(**SEM**).** Melt viscosity and mechanical properties of the composites and the blends were also measured. It was found that the clay spacing in the composites is influenced greatly by the type of polymer used. Also the addition of the nano-clay can greatly increase the viscosity of the polymer when there is a strong interaction between the polymer and the nano-clay. The mechanical test showed that the addition of 5-10 wt% nano-clay largely increases the elastic modulus of the composites. The water absorption of nylon 6 is decreased with the presence of nano-clay. The effect of nano-clay on polymers and polymer blends was also compared with Kaolin clay under the same experimental conditions.

Jong *et al.* (2002) investigate the mechanism of nanoclay exfoliation was investigated in epoxy-clay nanocomposites system. The elastic force exerted by cross-linked epoxy molecules inside the clay galleries was found responsible for exfoliation of clay layers from the intercalated tactoids. Complete exfoliation of clay galleries was observed under the conditions of slow increase of complex viscosity and fast rise of storage modulus. It was observed that faster intragallery polymerization, though expedited the exfoliation process, was not necessary for exfoliation. It was also observed that clays containing hydroxylated quaternary ammonium ions and quaternary ammonium ions with no polar functional groups produced exfoliated structures equally easily, provided the ratio of storage modulus to complex viscosity was maintained above 2-4 1/s. Both higher curing temperature and the presence of organically modified clay particles

accelerated the formation of gels, and the gel time presented an upper bound of time available for Exfoliation.

Isik *et al.* (2003) synthesized Diglycidyl ether of bisphenol A type epoxy resin-polyether polyol-organically treated montmorillonite ternary nanocomposites. The effects of addition of polyether polyol as an impact modifier on morphological, thermal and mechanical properties of nanocomposites were investigated by X-ray diffraction, scanning electron microscopy (SEM), differential scanning calorimetry, impact and tensile testing. The results showed that organically treated montmorillonite is intercalated by epoxy, since the interlayer spacing expanded from 1.83 to 3.82 nm upon nanocomposite synthesis. The addition of polyether polyol impact modifier had no effect on the interlayer spacing. SEM examination showed that polyol forms an immiscible phase in the epoxy matrix. In polyether polyol modified nanocomposites, the impact and tensile strengths decreased with respect to increasing amount of montmorillonite and showed a maximum with respect to the polyether polyol content at constant clay loading.

Sinha Ray *et al.* (2003) studied the academic and industrial aspects of the preparation, characterization, materials properties, crystallization behavior, melt rheology and processing of polymer/layered silicate nanocomposites. Smectite are a valuable mineral class for industrial applications because of their high cat ion exchange capacities, surface area, surface reactivity, adsorptive properties. Hectorite and montmorillonite are among the most commonly used smectite-type layered silicates for the preparation of nanocomposites. They suggested that these composites are generally exhibit improved mechanical properties compared to conventional composites. They exhibit a remarkable increase in thermal stability, as well as self-extinguishing characteristics for flammability, such that the flammability of pristine polymers are significantly reduced after nanocomposite formation with layered silicate.

Chun-Ki Lam *et al.* (2004) experimentally studied the hardness and inter-laminar shear properties of nanoclay/epoxy composites with different amount of nanoclay content, which formed different sizes of nanoclay/epoxy clusters after mixing in an extruder. The results showed that the micro-hardness of the composites could be enhanced when a small amount of nanoclay was added into the epoxy. However, there was an optimal limit in which the hardness was dropped by continuously increasing the nanoclay content. Microscopic observation on the

fracture surfaces showed that the size of the clusters varied with the amount of nanoclays used in the composites.

Chow *et al.* (2005) studied the water absorption and hygrothermal aging behavior of organomontmoiillonite (OMMT reinforced polyamide 6/polypropylene (PA6/PP ratio = 70/30)), with and without maleated PP (MAH-g-PP), at three different temperatures (30, 60, and 90^{o}C. The water absorption of the PA6/PP nanocomposites obeys the Fickian law behavior. It was found that the equilibrium moisture content and the diffusion coefficients are dependent on the OMMT loading, MAH-g-PP concentration and immersion temperature tensile modulus and strength of PA6/PP nanocomposites deteriorated after being exposed to hygrothermal aging. Water acts as a plasticizer for the PA6/PP matrix and silicate layer of OMMT. These nanocomposites showed excellent retention ability and recovery properties under any immersion temperature. The MAH-g-pp enhances the resistance of the nanocomposites against water immersion and also improved the resistance against hygrothermal attack.

Kornmann *et al.* (2005) synthesized and successfully used epoxy-layered silicate nanocomposites based on anhydride cured epoxy and octadecylamine modified fluorohectorite as matrix in glass-fiber-reinforced laminates by hand lay-up technique. The material used was the synthetic layered silicate Somasif ME-100. One hundred and twenty mille equivalents per 100 g of Somasif ME-100 of octadecylamine were dispersed in deionised water at 80^{o}C. They had done the flexural tests on the laminates and indicated that the presence of silicate layers in the epoxy matrix leads to a flexural strength improvement of 27%. According to dynamic mechanical measurements, the presence of organ silicate causes a decrease of the glass transition temperature. The glass transition temperature decrease is apparently responsible for the larger water uptake observed in the nanocomposite.

Beckry *et al.* (2005) were examined the properties of an E-glass/epoxy composite before and after mechanical loading and moisture conditioning. Preliminary results indicate that the modulus, strength, and strain of the E-glass/epoxy composite material are affected by the presence of moisture and mechanical loading when compared to control specimens. At shorter durations of conditioning at room temperature, a slight increase in strength and a slight decrease in modulus were observed; and at longer durations, 3000 h, a noticeable reduction in strength and strain-to-failure was observed. Specimens conditioned under stress, in water at 65^{0}C for

1000 h exhibited higher loss in modulus. It is speculated that constant stress may have a positive effect in short-term, and that extended exposure to moisture at room temperature leads to brittle failure while exposure at high temperatures may lead to ductile failure of E-glass/epoxy composites.

Yasmin *et al.* (2006) prepared the clay/epoxy nanocomposites by shear mixing. They use the 1-10wt. % of clay concentration to prepare the above samples. The epoxy matrix was reinforced with MMT clay particles to fabricate clay/epoxy nanocomposites. They used bisphenol A as epoxy resin and methyl tetrahydrophthalic anhydride as the hardener. Two types of clay nanoparticles were used as the reinforcement, one is Nanomer I.28E and other is Cloisite 30B. In this study Closite 30B shows a homogeneous dispersion of nanoparticles throughout the cross-section compared to Nanomer I.28E/epoxy. As the clay content increases, the strain to failure decreases. It was also found that the modulus of the nano-composites increases monotonically with increasing clay content. For 10 wt% of clay, the Cloisite30B/epoxy shows an increase of 53% over the neat resin, where as the other shows an increase of about 22% at room temperature. This observation further confirms the direct relation between the degree of exfoliation and the mechanical properties of these nanocomposites. The addition of clay also found to reduce the CTE (coefficient of thermal expansion) of pure epoxy.

Avila *et al*. (2006) used a set of fiber glass-epoxy-nanoclay laminate composites to investigate how the plate impact strength is affected by the presence of nanoclay. They prepared S2-glass/epoxy-nanoclay nanocomposites for this. The S2-glass/epoxy-nanoclay composite is a laminate with 16 layers and 65% fiber volume fraction. This type of configuration is prepared using a vacuum assisted lay-up technique. The amount of nanoclay added into an epoxy system, in weight, is 1%, 2%, 5%, 10%, respectively. To compare the results a set of S2-glass/epoxy laminated composites also prepared. The addition of nano-sized clays increases the composite impact strength, as the damaged area is decreased approximately 20% for small amounts of nanoclay contents. When the concentration reaches around 10% the increase on impact strength is near to 50%. Nano-clay composites show great performance over the conventional composites under the rebound/spring effect. When the four edge clamped condition is imposed the overall composite damping is increased with the nanoclay concentration. The most favorable nanoclay

concentration suggested by them close to be 5%. This can be due to the vibration mode superposition associated to a stiffness enhancement.

Avila *et al.* (2006) investigated the influence of montmorillonite (MMT) silicate layers on glass-fiber-epoxy laminated composites behavior by low-velocity impact and X-ray diffraction tests. The nanostructure laminate prepared for this investigation is a S2-glass/epoxy-nanoclay. The nanoclay is used in this was Nanomer I30E. The amount of nanoclay dispersed into the epoxy system, in weight, is 1%, 2%, 5%, 10%, respectively. As the amount of nanoclay dispersed gets bigger, there is an increase in stiffness. As the stiffness reaches its peak value, the fracture toughness and damping were reduced. Specimens with 5% nanoclay content were shows the best performance with respect to damping. As the energy increases, the nanostructure laminate response gets weaker. When the low-velocity impact results were analyzed they showed an increase on energy absorption close to 48% for low energies, 20 J, 15% increase for medium–high energies, 60 J, and 4% for high energy, 80 J. As the amount of intercalated nanoclay content varied from 0% to 10%, the optimum condition for low-velocity impact seems to be around 5%.

Wetzel *et al*. (2006) studied the manufacturing and the characterization of epoxy nanocomposites. Special attention was directed towards reinforcing effects of nanoparticles on the polymer toughness. The incorporation of both Al_2O_3 and TiO_2 nanoparticles into the epoxy resin improved flexural stiffness, flexural strength, and fracture toughness of the polymer at the same time. Cracks in Dynamically loaded nanocomposites propagated at lower rates than in neat epoxy. The fillers were well bonded to the matrix, which was indicated by both the shift of the glass transition temperature to higher temperatures and the increase in the rubbery plateau modulus. Moreover, the presence of Al_2O_3 in epoxy increased the apparent yield stress, the yield strain, and the size of the plastic zone. Debonding effects in the process zone, as often observed in glass bead filled epoxies, are rather unlikely to participate in the toughening of EP/Al_2O_3 nanocomposites, due to the small dimensions of fillers. Further investigations will help to find relationships especially between the morphology, the relevant toughening mechanisms, and the toughness of EP/Al_2O_3 nanocomposites. It is believed that the observed property characteristics are related to the influence of nanoparticles on the molecular structure of the matrix itself.

Wang *et al.* (2006) studied the effects of hydrothermal ageing on the thermo-mechanical properties of high performance epoxy and its nanocomposite. In this work epoxy–clay

nanocomposite samples containing 2.5 wt% of clay were prepared through a "slurry-compounding" approach. The cured samples were immersed in distilled water at 60°C for different periods of time before subjecting to characterization. The hydrothermal effect on the thermal/mechanical properties of neat epoxy and epoxy–clay nanocomposite was studied. The moisture uptake significantly affects the modulus at high temperature, the tensile strength, and the α-relaxation behavior. On the other hand, at low temperature, the modulus and fracture toughness were not strongly influenced. As the moisture content increases, there is a reduction in strain at break for the epoxy–clay nanocomposite while that of the neat epoxy remains constant. This effect was attributed to epoxy–clay interface debonding induced by water and formation of water cluster fillers that act as defects in the composite.

Berketis *et al.* (2007) investigated the matrix and fiber/matrix interfacial degradation of glass fiber composites subjected to water for very long time. Laminated composite plates were manufactured by the vacuum assisted resin transfer molding technique. The resin used was the polyester (crystic 489 PA). This paper examines the durability of an isopthalic polyester resin reinforced with non-crimp glass fabrics in a hydrothermal environment for up to 30 months. The weight of the composite plates initially increased due to water diffusion up to month 14 and thereafter decreased due to material losses. The initial weight increase was due to diffusion of water into the specimens. Immersion in water also resulted in significant de-bonding of the fiber/matrix interface, which allows water to penetrate the composite material by capillary action. The impacted plates were retested statically to determine residual compressive strengths for the assessment of damage tolerance. A new device was designed for the CAI tests that assured laminate failure by de-lamination propagation. The results of the CAI testing demonstrated a reduction in CAI strength, due to hydrothermal exposure for each applied level of impact loading. Immersion time of 24 and 30 months showed that a local plateau was approached in CAI strength.

Quaresimin *et al*. (2007) worked on the effect of three different commercially available nano-modifiers on the mechanical properties of an epoxy/anhydride unidirectional carbon fiber reinforced laminates. The polymeric matrix consisted of a blend of the diglycidyl ether of Bisphenol A and the epoxy novolac resin. The hardener was a hexa-hydrophthalic anhydride. The nanoclay used here was Cloisite 30B. The organo-clay was dispersed through a shear mixing

process. Hand-layup method is used to prepare the specimens. The work had shown that tensile modulus exhibited little difference between the unmodified laminates while a modest decrease was observed for the tensile strength for the VGCF (vapors grown carbon fiber) and nanoclay modified systems. The result being that the ‘‘effective’’ clay concentration in the interlayer resin rich regions was much higher than the nominal nano-additive concentration.

Shang-Lin *et al.* (2007) performed experimental investigation of nanocomposite coatings for healing surface flaws of glass fibers and improving alkali-resistance. He found that, with low fraction of nano-reinforcements, the nanostructures and functionalized traditional glass fibers show significantly improved both mechanical properties and environmental corrosion resistance. The most remarkable mechanical strength improvement is found for glass fibers with nanotubes coatings, corresponding to the highest healing efficiency factor. No apparent strength variation appears for nanoclay coated fiber subjected to alkaline attack, which indicates that, the influence of moisture solvent uptake and concentration on mechanical properties decreases when the organoclay is dispersed in coating polymer. Overall, the hybrid nanocoatings cause improved fiber strength, corrosion resistance, and interfacial properties.

Chow *et al.* (2007) has prepared the epoxy/glass fiber/organo-montmorillonite (OMMT) nanocomposites by hand lay-up method. In this work, the epoxy nanocomposites were characterized by X-ray diffraction (XRD), differential scanning calorimetry (DSC) and water absorption tests. Epoxy/glass fiber/OMMT hybrid nanocomposites prepared by hand-layup technique showed exfoliation characteristics and slightly enhancement in glass transition temperature. The water resistance properties of epoxy were improved by the addition of both glass fiber and OMMT, which is maybe attributed to the increasing of the tortuosity path for water penetration.

Paul *et al.* (2008) states that exfoliated clay-based nanocomposites have dominated the polymer literature but there are a large number of other significant areas of current and emerging interest. This review will detail the technology involved with exfoliated clay-based nanocomposites and also include other important areas including barrier properties, flammability resistance, biomedical applications, electrical/electronic/optoelectronic applications and fuel cell interests. The important question of the ‘‘nano-effect’’ of nanoparticle or fiber inclusion relative to their larger scale counterparts is addressed relative to crystallization and glass transition behavior. Of

course, other polymer (and composite)-based properties derive benefits from nanoscale filler or fiber addition and these are addressed.

Manjunatha *et al*. (2009) tests the tensile fatigue behavior of a silica nanoparticle-modified glass fiber reinforced epoxy composite. The epoxy resin was a standard diglycidyl of Bisphenol A with an epoxide. The GFRP composite laminates were manufactured by resin infusion under flexible tooling technique. An anhydride-cured thermosetting epoxy polymer was modified by incorporating 10 wt. % of well-dispersed silica nanoparticles. The fatigue life of 10 wt. % silica nanoparticle-modified bulk epoxy is about three to four times higher than that of neat epoxy. The fatigue life of the GFRP composite with 10 wt.% silica nanoparticle modified epoxy matrix is about three to four times higher than that of the GFRP with the neat epoxy matrix. The suppressed matrix cracking and reduced crack growth rate due to the particle debonding and plastic void growth mechanisms appears to contribute for the observed enhancement of the fatigue life in the GFRP with the nanoparticle-modified matrix.

Maitra *et al*. (2009) shows that PVA polymer-matrix composites reinforced with small concentrations of functionalized ND were synthesized and evaluated. Detailed structural characterization, employing a variety of analytical techniques, shows that the nanoparticles are distributed uniformly and do not agglomerate. Further, they appear to interact with the polymer matrix strongly, increasing the crystallinity substantially. The mechanical properties of the PVA-ND composites are determined using nano-indentation technique. With only 0.6-wt% addition of ND, which is relatively small, significant enhancements to the hardness and Young's modulus of the PVA were observed. It was suggested that excellent adhesion between the matrix and the functionalized ND particles is the main reason for this marked improvement in mechanical performance. These results indicate that ND can be successfully used as a filler material for making polymer composites.

Zainuddin *et al*. (2010) was shown here that E-glass epoxy fiber reinforced composite was sensitive to environmental conditioning especially under hot-wet conditions. The weight gain was higher for all the wet conditions samples exposed to elevated temperatures. Addition of 1–2 wt% of nanoclay decreased the weight gain. Flexural properties were found to degrade with increase in time. 2 wt% GFRP composites showed enhancement in properties under all conditions over neat counterparts. In some cases, samples subjected to hot dry condition at 60^0C

showed increase in properties over room temperature conditioned samples. Scanning electron micrographs provided clear evidence of the effects of nanoclay, elevated temperature and moisture absorption. Enhancement in interfacial bonding was observed in 2wt.% composite samples, both at room temperature and hot-wet conditioning.

Singh *et al.* (2010) reports on the durability of epoxy-clay nanocomposites upon exposure to multiple environments. Nanocomposites are fabricated by mixing the clay particles using various combinations of mechanical mixing, high-shear dispersion, and ultrasonication. Clay morphology is characterized using X-ray diffraction and transmission electron microscopy. Specimens of both neat epoxy and the epoxy-clay nanocomposite are subjected to two environmental conditions: combined UV radiation and condensation on 3-hour repeat cycle and constant temperature-humidity, for total exposure duration of 4770 hours. Both materials lose mass under exposure to combined UV radiation and condensation due to the erosion of epoxy by a synergistic process. Surprisingly, the epoxy-clay specimens exhibit greater mass loss, as compared to neat epoxy. Mechanical testing shows that either environment does not significant affect the flexure modulus of either material. On the other hand, both materials undergo degradation in flexural strength when exposed to either environment.

CHAPTER 3 RESEARCH PROBLEM

3.1 Gaps in literature

From the literature review it is found that work so far reported in literature has been mainly focused on the synthesis of polymer nanocomposites and the characterization of the mechanical properties. There are no detailed studies on nanoclay addition to the epoxy matrix for preparing FRPs and then carrying out the hygrothermal studies. Some of the following gaps in the previous research are:

1. There are still difficulties in distributing nanoparticles homogeneously in the matrix.
2. Most of the work is focused on synthesis and characterization and not on hygrothermal aging studies of epoxy based FRP.
3. Very few reports on the use of these nanocomposites as matrix in fiber-reinforced composites.

3.2 Research Problem

The present study is mainly focused upon the synthesis of epoxy layered silicate nanocomposites as matrix in fiber reinforced composites, their characterization and determining the mechanical properties. The durability studies have been carried out by placing the specimens, with different clay loading, in water and alkaline medium for a period of one month.

CHAPTER 4 FABRICATION & EXPERIMENTATION

4.1 Work Plan

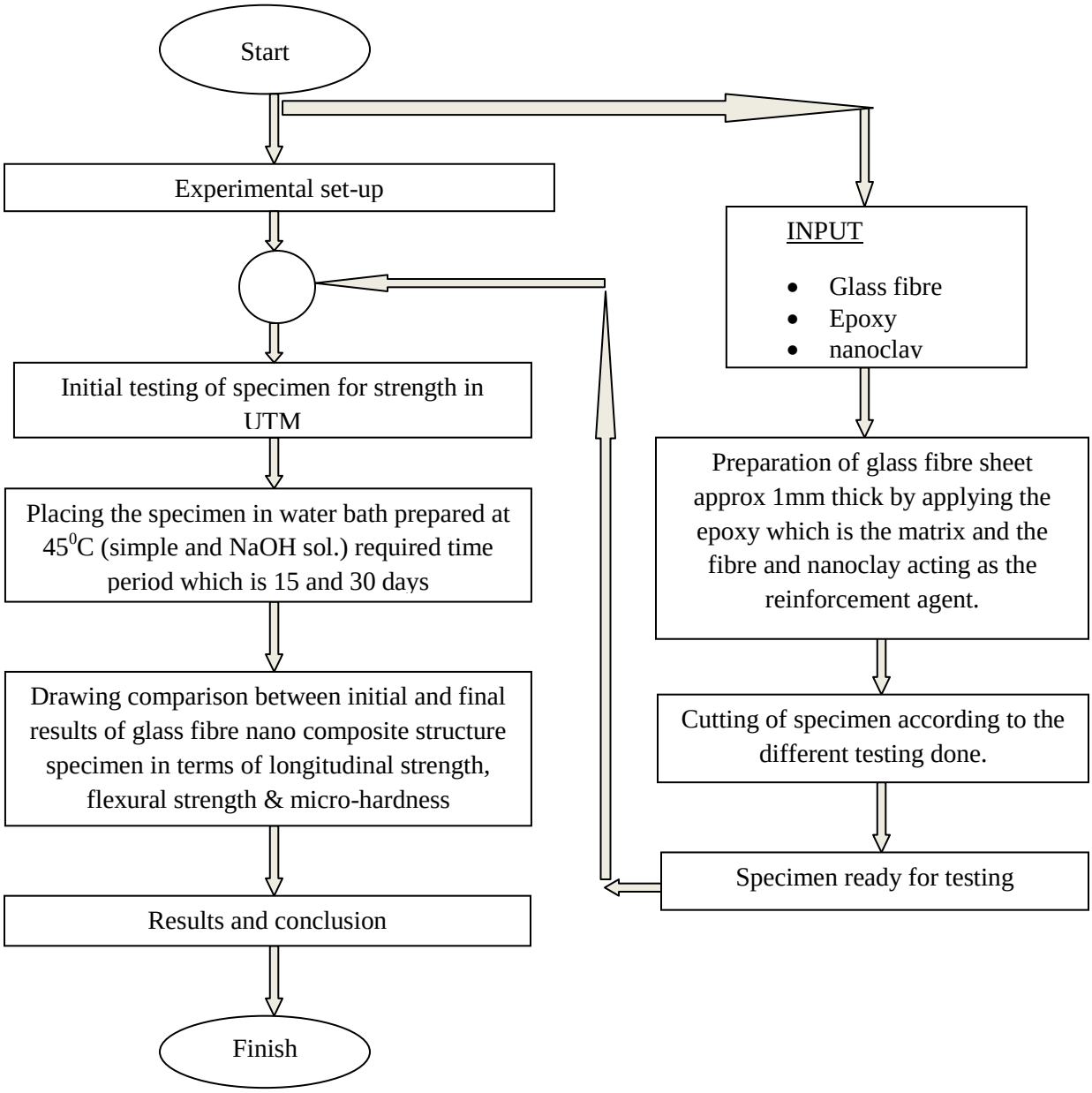

4.2. Fabrication of Specimen

4.2.1. Materials

Unidirectional E-glass fibre and M Brace a two part epoxy resin purchased from **BASF Construction Chemicals (India) Private Limited**. Organically modified nanoclay Closite 30B purchased from **Connell Bros. Mumbai.**

4.2.2. Specimen Specifications

Commercially available glass fiber mat had been used for making specimen. The sheets were placed along 0^0 orientation side for cutting the specimen. The specimen had been cut and prepared as per the ASTM standards D3037/3039 and D790 for tensile and bending tests respectively. The dimensions of specimens are shown below.

Table 4.1 Specimen Specifications for Testing

Parameters for specimen	Specimens for tensile testing	Specimens for Flexural testing
Length	250 mm	125 mm
Width	15 mm	12.7 mm
Thickness	1.5 mm	1.5 mm
Tab length	56mm	-
Tab thickness	0.8mm	-

4.2.2.1. Specimen Dimensions

- **For bending test**

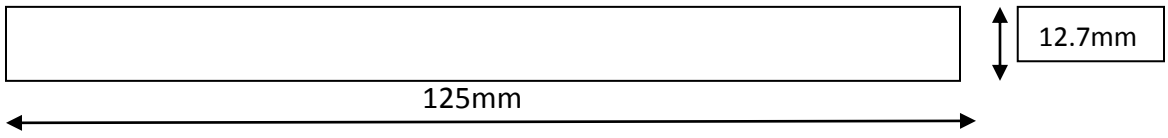

Fig.4.1 Specimen dimensions for bending test

Fig.4.2 Nanocomposite bending specimen

- **For tensile test**

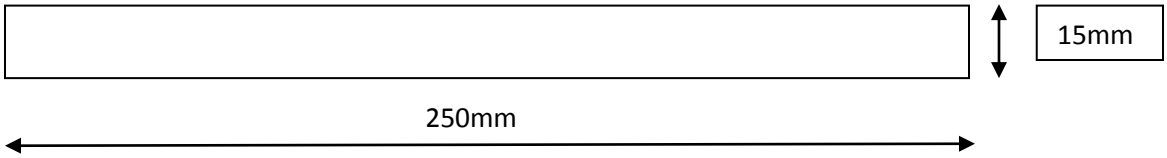

Fig.4.3 Specimen dimensions for tensile test without tabs

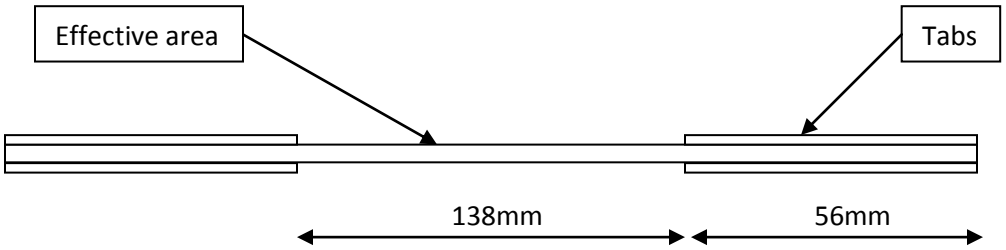

Fig.4.4 Specimen dimensions for tensile test with tabs

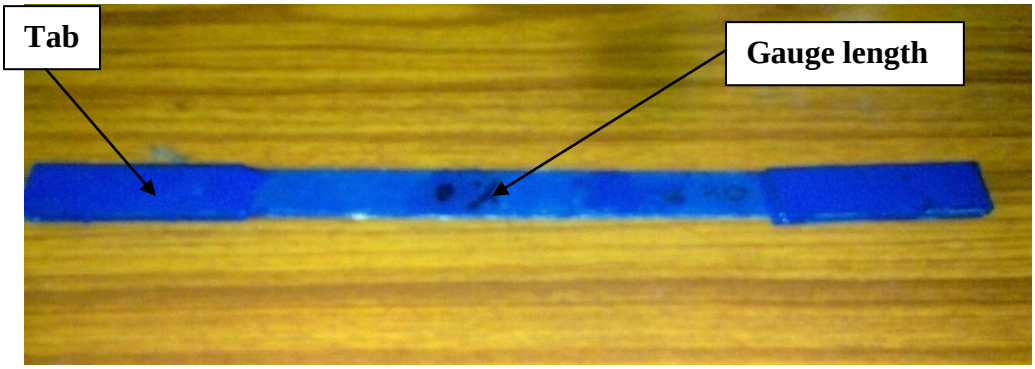

Fig.4.5: Nanocomposites specimen for tensile testing

4.2.3. Cutting Glass Fiber Sheet

For the experimentation unidirectional roll of glass fibre was purchased having 50cm width having 0^o fibre orientation woven with polymer fibers. The sheets were initially cut from roll in lengths of 450 mm (Fig. 4.6).

Fig. 4.6 Uncoated glass fibre mat used for making specimen

4.2.4. Mixing of Nanoclay into Epoxy (base):

- **Mechanical stirring**: Epoxy base is a blue colour thick fluid. It is quite difficult to mix nano silicates into it manually. So we used a mechanical stirrer and an oil bath for proper mixing of nanoclay (Fig. 4.7). Oil bath was used to heat up the epoxy to desired (60^0 C) temperature, so the viscosity of epoxy base is reduced. Proper mechanical stirring of epoxy at this stage resulted better dispersion of clay.

Fig. 4.7 Oil bath set-up with mechanical stirrer

Different weight percentages of clay - 1, 3 and 5 % by weight of epoxy, were added and stirred at a temperature of 60^0C for 2 hours.

- **Ultrasonication after Mechanical Stirring:** Sonication is the act of applying sound energy to agitate particles in a sample, for various purposes. In the laboratory, it is usually carried out using an ultrasonic bath or an ultrasonic probe, colloquially known as a sonicator. Sonication can be used to speed dissolution, by breaking intermolecular interactions. Sonication was done for evenly dispersing nanoparticles in liquids. After mechanical stirring of the epoxy solution container was placed into the ultrasonication bath for up to 2 hours.

Fig.4.8: Ultrasonication bath

4.2.5 Mixing of Epoxy Base Solution with Hardener:

After ultrasonication, the solution is mixed with the hardener in the ratio 10:4 by volume. After mixing, manual stirring up to 5 to 10 minutes was done. The whole procedure is shown in Fig. 4.9.

Fig. 4.9 mixing of hardener to the base component

4.2.6. Coating of Nanoclay mixed Epoxy to Glass Fiber Sheets:

The mixture was then poured on to the glass fibre mat and applied uniformly using the hand layup method. For this, steel scraper was used to maintain uniformity of the solution. It was made sure that there is no air bubbles entrapped inside the epoxy applied on sheet otherwise it would create a flaw there. After applying epoxy, the sheet took overnight to dry and then coating was done on other side following same procedure. The full curing of sheet (Fig .4.10 & Fig. 4.11.) was done by leaving it under ambient temperature for at least seven days before processing further.

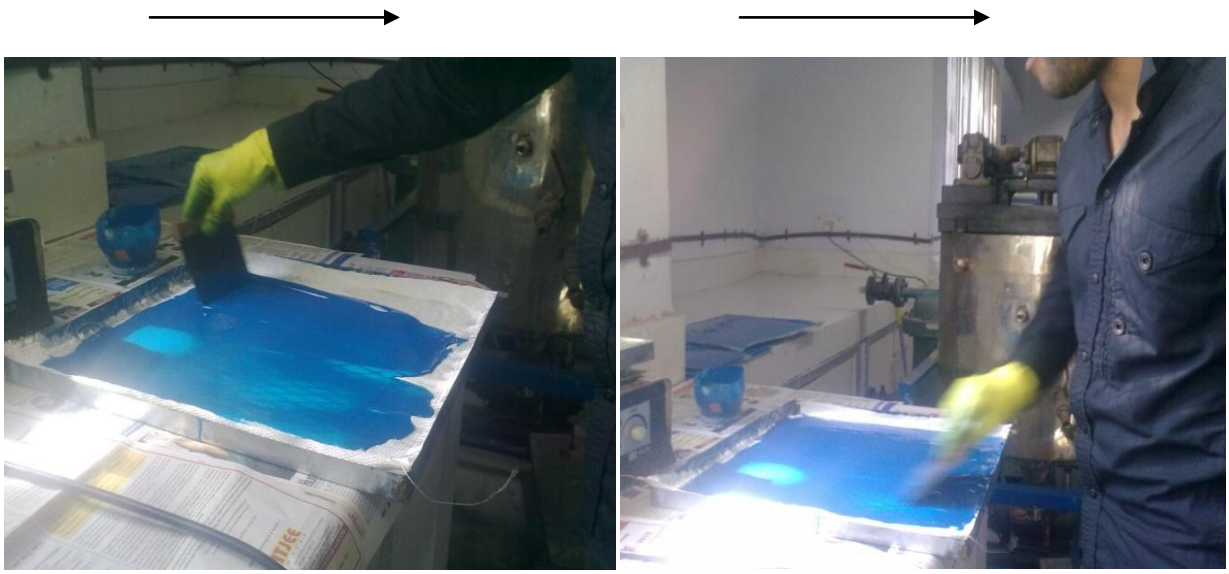

Fig. 4.10 Coating the glass fiber sheet with epoxy solution

Fig. 4.11 Coated sheets placed for curing

4.2.7. Sizing of Sheet for Samples and Tabs

Once the epoxy was fully cured, cut the sheet to actual sample size using the Treadle shearing machine (Fig. 4.12) which would shear it into required size. The tabs were also cut with same Treadle shearing machine (Fig. 4.13 & Fig. 4.14).

Fig. 4.12 Treadle Shearing Machine

Fig. 4.13 Samples before tabbing

fig. 4.14 Actual image of "Tab"

4.2.8. Placing Tabs on Samples

The samples had to be tabbed on either side on two ends. We had to prepare the mixture of epoxy and carefully apply it on the either side of sample. The tabs were now placed on either side of epoxy pasted sample (with epoxy coated side of tab on upper side). The epoxy would act as binder between tab and actual sample.

Fig. 4.15 Sample tabbed, Clamped and left for drying

Two paper clamps were placed on either tabbed side to hold tabs in place and also to apply pressure while epoxy between them was getting dried (Fig. 4.15). Once the sample was dried, paper clamps used to hold tabs in place were removed. Samples were again cured for 5 days before they were put to any testing. A single sample finally would have four tabs (in total) on either side of both ends. This sample was ready now for any kind of further testing.

4.3. Experimental Set-up

A set of accelerated aging tests had been carried out to evaluate performance of glass fibre reinforced polymer (GFRP) sheets embedded in epoxy matrix. The field environment very similar to that of tropical climate had been simulated. The specimens were immersed in two water baths for different time durations.

Fig. 4.16 Setup view of the water baths

The specimens were removed from the bath after an interval of 15 days. The tensile and flexural strength was measured to check the degradation in properties of composite material. Both of the water tanks were filled with water. One was of simple water and other tank was containing NaOH 5% by weight of water. Both the tanks were kept at a temperature of 45^0C.

4.3.1. Setup Fabrication:

Table 4.2 Shows that the set-up basically consists of following main items

S.No.	ITEM NAME	QUANTITY
1	Water tanks	02
2	Specimens	64
3	Heating Elements	02
4	RTD Sensors	02
5	Temperature Controllers	02

4.3.2. Water Tanks:

The experimental setup consists of three well insulated tanks (Fig. 4.16). The tank was of cylindrical shape made out of plastic. The approximate capacity of the tank was 60 liters. Both the tanks were filled totally with tap water and set at a temperature of 45°C. NaOH was added to one tank (5% by weight of water). The water which evaporated from the tank was replenished on daily basis during experimentation. Each tank was labeled as per details of experimentation.

4.3.3. Heating Element:

The setup was heated with help of commercially available heating rod elements (Fig. 4.17). Each bath was having its own heating rod connected via temperature controller (Fig.4.18). The wattage of rod was 1000KW with single phase connection. As the temperature reached the required value the power supply of rods were cut off by controllers.

Fig. 4.17 Heating Element and RTD sensor in a tank

4.3.5. Temperature Controller:

The objective of this set up was to maintain the bath temperature at specified value till the duration of experiment for day and night on daily basis. So a temperature controller (Fig.4.18) was connected with each of the bath along with relays cut off. The controller used the proportional-integral-derivative (PID) control to maintain the temperature. On the controller display the "Set Value" was given which was the temperature indicated in green and the "Process Value" of temperature was indicated in the red (refer Fig.4.18), which was the output from the RTD sensor. For the very first time the controller was set to auto-tune mode so that it could adjust itself according to the input variables. Once the bath had attained the set value the controller cut off its supply and after sometime it sensed the temperature if it had gone below set value, it again started heating to obtain the set value. The dimensions of the controller and actual panel used are shown in Fig.4.18 and Fig. 4.19 respectively.

Fig. 4.18 temperature controller

Fig. 4.19 Temperature display panel with controller

4.4. Testing Methods used in Experimentation

4.4.1. Tensile Testing

A Universal Tensile testing machine shown in Fig.4.20 and Fig.4.21 was used for the testing of the FRP specimen for its tensile strength. The test specimen had been prepared according to ASTM-D-3039 standard. The specimen were tested until they break indicating the peak load and ultimate stress value they can bear at required time period to estimate the degradation in the same machine.

Fig. 4.20 UTM testing machine

Fig. 4.21 Specimen in jaws

4.4.2. Three Point Flexural Test

Three point bending tests of specimen were carried out in using Zwick / Roell (Fig. 4.22).

Fig. 4.22 Three point bend test machine

Fig. 4.23 Specimen positioning

The test specimen had been prepared according to ASTM-D-790 standard. The three point bending test results can be taken as indications of strength degradation of composites after they had been hygrothermally treated.

4.4.3. Micro Hardness Test

Micro hardness test (shown in Fig.4.24) was conducted on specimen with different clay loadings to see the effect of clay loading on hardness values.

Fig. 4.24 Micro hardness equipment

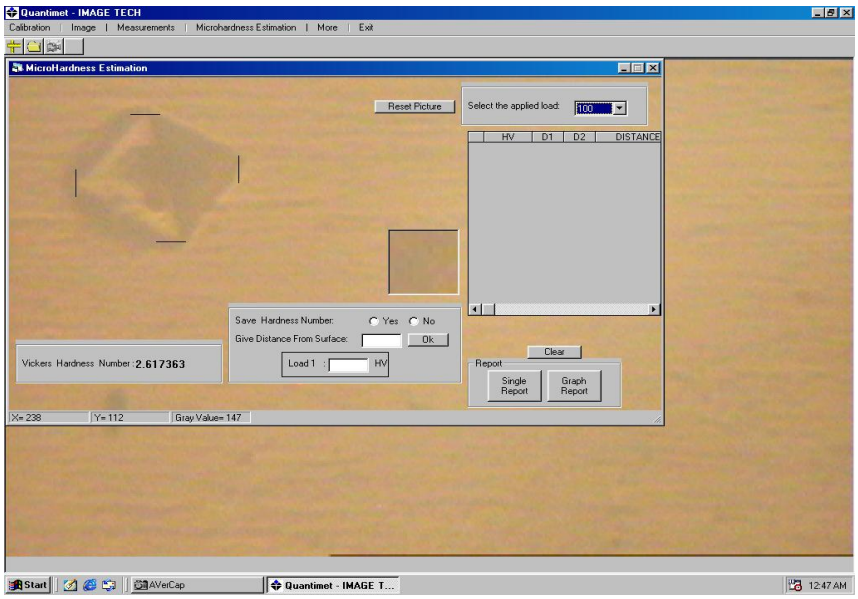

Fig. 4.25 Indent of specimen

The load applied was 200gm and VHN values were determined by applying this load by using a calibration distance of 50 units in Quantinet software as shown in Fig.4.25 used for image analyzing. The dwell time used during load application was 20 seconds. An indent is formed in diamond shape used for calculating VHN as shown in figure below.

4.4.4. SEM (Scanning Electron Microscope)

Scanning electronic microscope shown in Fig.4.27 was used to test FRP specimen microstructure. The dimensioning of specimen was done according to block size of machine. The polishing of specimen was done by using Gold coating equipment as shown in the Fig.4.26. The polished specimen was used to observe the microstructure of specimen at different magnification.

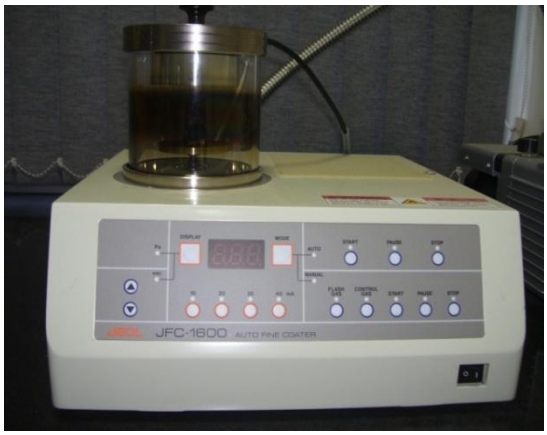

Fig. 4.26 Gold coating equipment

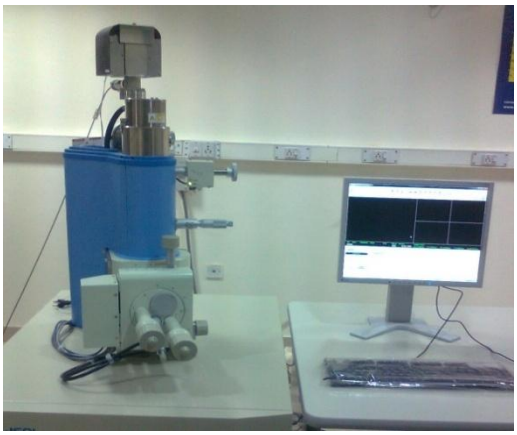

Fig. 4.27 SEM machine

SEM micrographs are helpful in viewing the micro-structure of material, hence showing any changes in physical structure of material and showing any defects like cracks, voids generated after loading of clay and hygrothermal degradation of the material. These are also helpful in calculating the area fraction of fibre and epoxy in the given specimen and the changes occurring and for also calculating the circularity of the fibre in case of GFRP.

4.4.5. Rockwell Hardness Tester

The Rockwell scale is a hardness scale based on the indentation hardness of a material. The Rockwell test determines the hardness by measuring the depth of penetration of an indenter under a large load compared to the penetration made by a preload. There are different scales, which are denoted by a single letter, that use different loads or indenters.

The determination of the Rockwell hardness of a material involves the application of a minor load followed by a major load, and then noting the depth of penetration, hardness value directly from a dial, in which a harder material gives a higher number. The chief advantage of Rockwell hardness is its ability to display hardness values directly, thus obviating tedious calculations involved in other hardness measurement techniques.

4.4.6. X-Ray Diffraction Test

X-ray scattering techniques are a family of non-destructive analytical techniques which reveal information about the crystallographic structure, chemical composition, and physical properties of materials and thin films. These techniques are based on observing the scattered intensity of an X-ray beam hitting a sample as a function of incident and scattered angle, polarization, and wavelength or energy.

X-ray diffraction was used in this study to investigate the crystallographic structure of the epoxy nanocomposites. XRD will enable the changes that occur to the clay due to the intercalation and/or exfoliation of the epoxy into the clay galleries to be quantified. The d-spacing of the inter-gallery spacing can be determined using Bragg's Law:

$$\lambda = 2d\sin\theta$$

Where λ is the wavelength of the incidence x-ray source, d is the spacing in question, θ is ½ of 2θ the Bragg angle or the diffracted angle of the incidence x-ray beam. Below is a schematic of the previously mentioned Bragg's Law (Fig. 4.28).

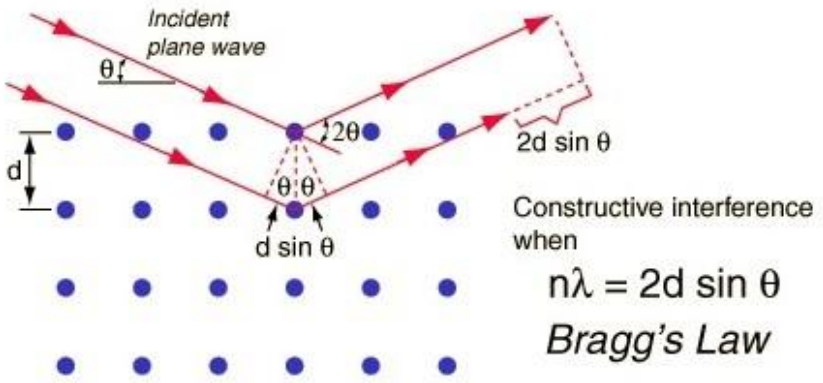

Fig. 4.28 Schematic representation of x-ray diffraction principle and the Bragg Law

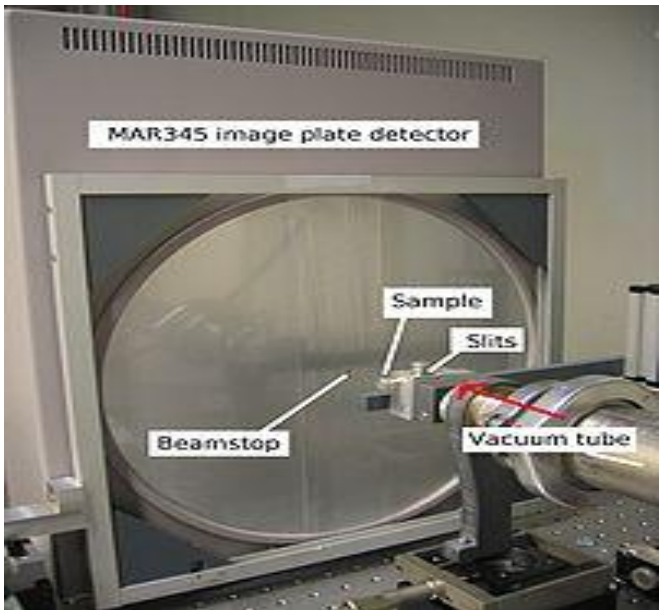

Fig.4.29 Schematic representation of x-ray Diffractometer principal

To evaluate the degree of exfoliation in the polymer, XRD measurements were carried out in a Panalytical X-ray diffractometer with Cu Kα radiation (λ=1.54Å) with a scanning speed of 1^0/min and at 45 kV and 40mA. During the XRD experiments, the samples were analyzed in reflection mode. All XRD scans were through 2θ of 0^o to 32^o.

4.5 Test Matrices

Table 4.3 Initial Testing Specimens

Specimen name	No. of specimen		Total specimen
	Tensile	bending	
0 wt%	2	2	4
1 wt%	2	2	4
3 wt%	2	2	4
5 wt%	2	2	4
Total specimen			**16**

Table 4.4 Distribution of above GFRP Nano Composite Specimen for Accelerated Degradation in 45°C Simple Water Bath

Specimen	Tensile		flexural		Total
	15 days	30 days	15 days	30 days	
0wt%	2	2	2	2	8
1wt%	2	2	2	2	8
3wt%	2	2	2	2	8
5wt%	2	2	2	2	8
Total specimens					**32**

Table 4.5 Distribution of above GFRP Nano Composite Specimen for Accelerated Degradation in 45°C NaOH Solution (5% by weight of water)

Specimen	Tensile		Flexural		Total
	15 days	30 days	15 days	30 days	
0wt%	2	2	2	2	8
1wt%	2	2	2	2	8
3wt%	2	2	2	2	8
5wt%	2	2	2	2	8
Total specimens					**32**

CHAPTER 5 RESULTS AND DISSCUSSION

5.1 MICROSCOPIC BEHAVIOR

5.1.1 Micro-Hardness

5.1.1.1 Specimen for Micro Hardness

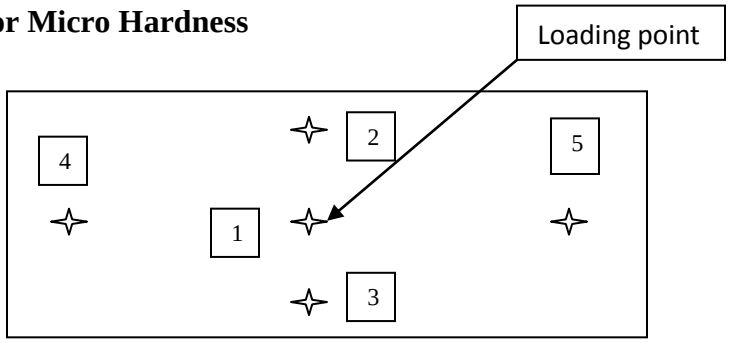

Fig. 5.1 showing different loading points in specimen

The micro-hardness of specimen at different clay loading was measured. The table 5.1 shows the experimental measurements of micro hardness of the nanocomposites with different nanoclay contents. An average hardness was calculated by 5 indentation measurements and a plot of the results of each type of samples is shown in Fig. 5.2.

Table 5.1 Micro Hardness Values for Different Clay Loading Samples

Clay loading / loading points	Micro hardness values			
	0 wt%	**1 wt%**	**3 wt%**	**5 wt%**
Point 1	2.443195	2.617363	2.736999	2.290125
Point 2	2.122409	2.752528	3.056269	2.546532
Point 3	2.588681	2.602963	3.038104	2.403509
Point 4	2.056269	2.967040	3.002257	2.452007
Point 5	2.326049	2.832192	3.093091	2.519002
Average	**2.297217**	**2.734027**	**3.032210**	**2.458172**

The maximum hardness has been measured where the nanoclay content reached 3 wt%. A decline of the hardness also appears on further increasing the nanoclay content; the hardness decreases in a drastic manner from 3.03 Hv (3 wt% of nanoclay) to 2.45 Hv (5 wt% of nanoclay). In most previous literatures, it has been indicated that adding a small amount of nanoclays into polymer-based materials could potentially enhance their strength, like hardness of the current samples with the nanoclay content less than 5 wt%. However, it is also reasonable to believe that it should have an optimal limit since the physical properties between these nano-structural materials and matrix are different. In the current study, it was demonstrated that the hardness was dropped if the amount of the nanoclays was beyond 3 wt%. It was suspected that the nanoclays might retard the chemical reaction, and so cause incomplete curing process of the composites. For all samples with high nanoclay content, the matrix might not be fully cured.

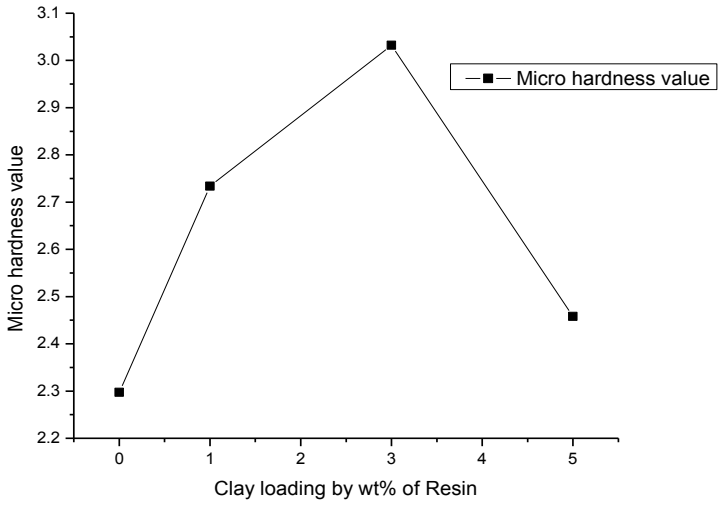

Fig. 5.2 micro hardness values at different clay loading

5.1.2 X-ray Diffraction Test

The X-ray Diffraction experiments were conducted on the samples having different nanoclay loading. X-ray diffractometer gives the values of d-spacing and 2θ for different samples of epoxy clay nanocomposites. The d-spacing values and Bragg`s angle values of the different samples are given in Table 5.2. An increase of the interlayer distance leads to a shift of the diffraction peak toward lower angle. The diffraction peak of Closite 30B comes out at an angle **2θ = 4.8452**

having d-spacing value is **d** = **18.26854**, Hence the shift in angle to the lower side shows the increase in d-spacing.

Table 5.2 shows the angle 2θ and d-spacing values of the Closite 30B and the epoxy nanocomposite having different clay loading 1wt%, 3wt% and 5 wt% respectively. From this table it is clear that as the angle 2θ shifts to lower the d-spacing value increases this means the nanocomposite are made.

Table 5.2 d-spacing of Clay and Epoxy Layered Silicates Nanocomposites

S.No.	Clay loading	Angle (2θ)	d-spacing (Å)
1	Closite 30B	4.8452	18.26854
2	1wt%	2.7170	32.51781
3	3wt%	2.7123	32.57421
4	5wt%	2.3214	38.05891

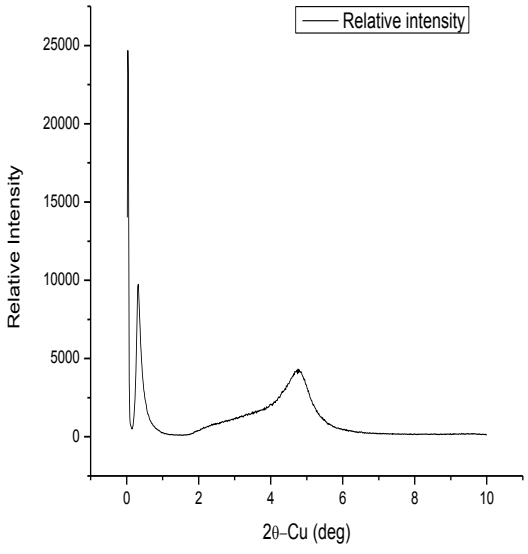

(a)

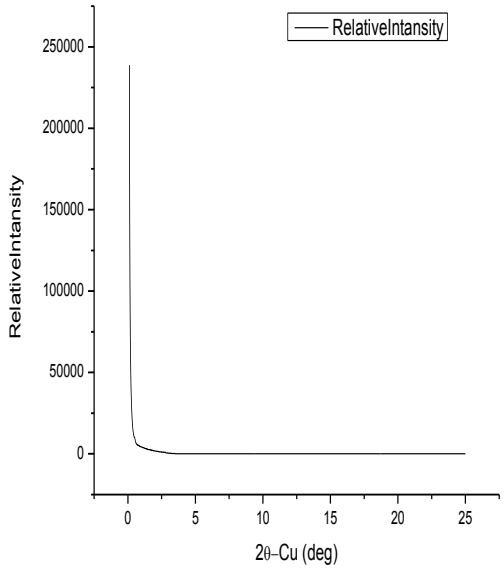

(b)

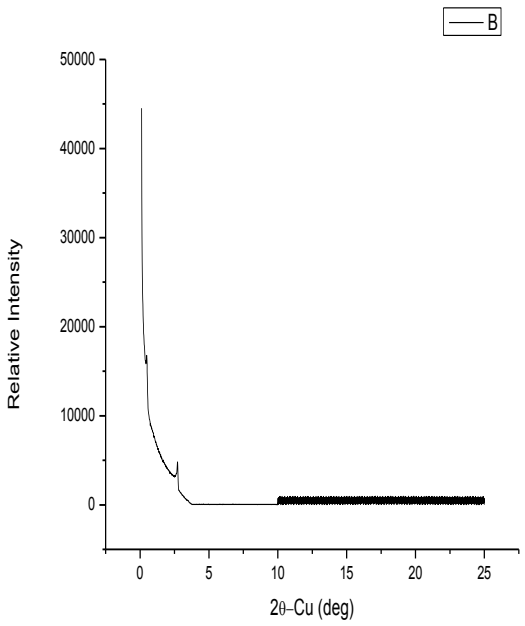

(c)

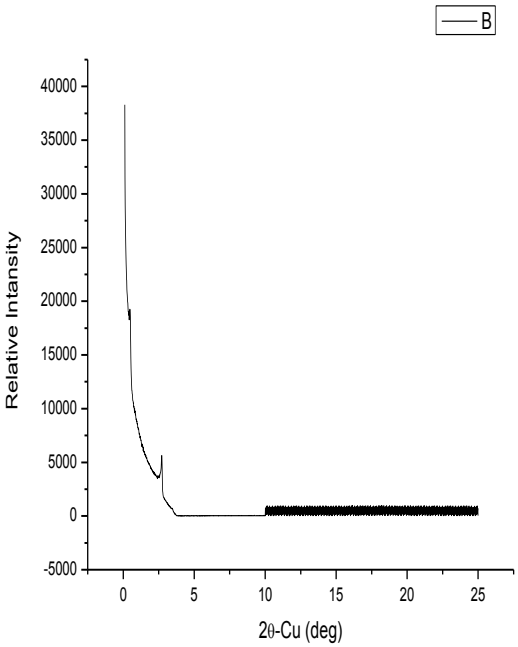

(d)

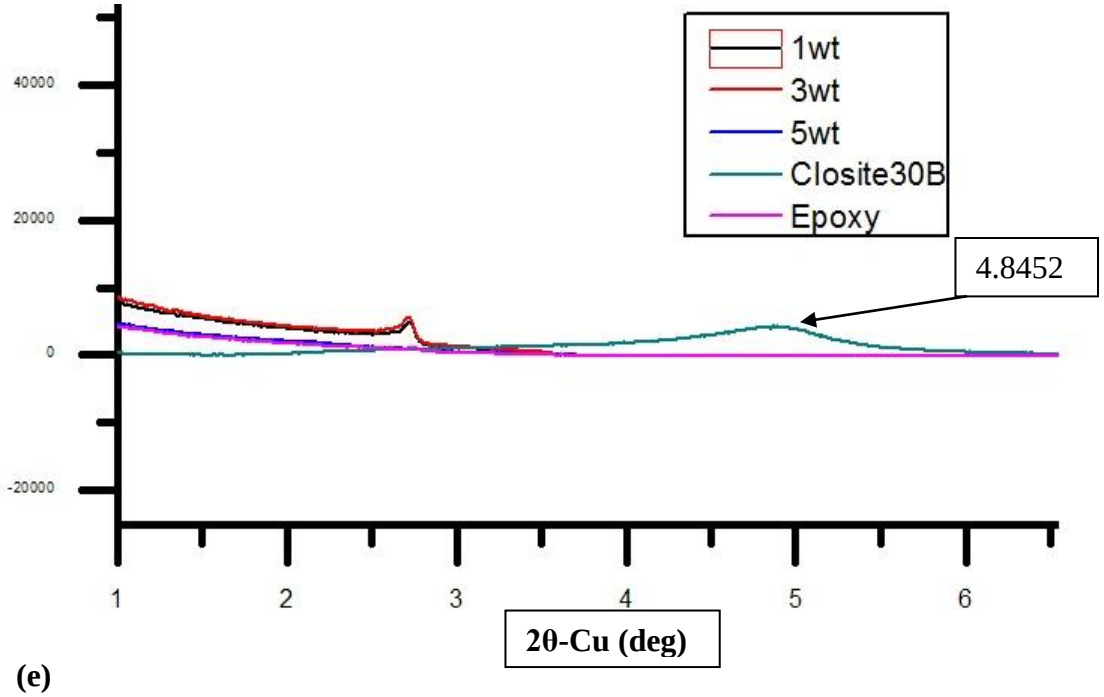

(e)

Fig.5.3 X-ray Diffractogram (a) Closite 30B (b) Epoxy Resin (c) 1wt% nanoclay (d) 3wt% nanoclay (e) graph showing peaks for all clay loadings

Fig.5.3 shows the X-ray Diffractogram of an epoxy-layered silicate nanocomposite prepared with 0 wt%, 1 wt%, 3 wt% and 5wt% of Closite 30B clay. Due to the polymerization of the epoxy between the silicate layers, the peak corresponding to the interlamellar spacing of the layered silicates has been shifted towards lower angle.

5.1.3 Scanning Electron Microscope (SEM)

SEM was used to determine size and distribution of particles in the samples for the four polymer nanocomposite systems. The primary goal of using SEM was to determine particle dispersion. Scanning electron microscopy was used in this study to obtain high magnification photos of the gfrp nano composites to observe their structures in order to relate with the resulting properties. Images of several different clay loading samples were obtained at magnifications ranging from 100X to 6000X.

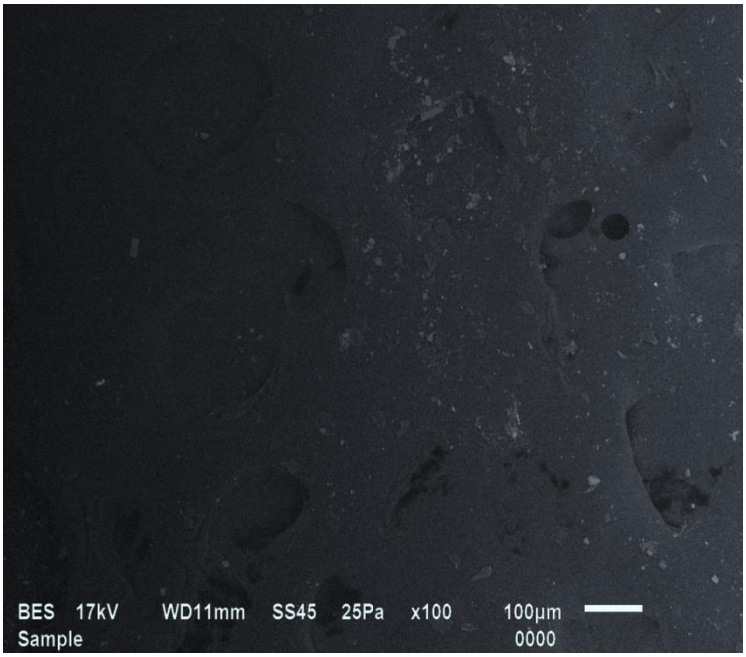

Fig. 5.4 SEM image of pure epoxy at 100x

In fig. 5.4 the SEM image of epoxy composite at 100 x has been shown. In comparison to pure epoxy, after 1 wt% clay addition (Fig. 5.5) the clay dispersion has been observed at different magnifications. Many particles of varying sizes are visible, appearing as small bright dots, fairly well dispersed across the image. Fig. 5.5(a) & (b) shows the particle dispersion at 100x and

4000x respectively. It has been observed that the particles are dispersed in the matter, when it observed at higher magnification the particles are looks like a small cluster of silicates.

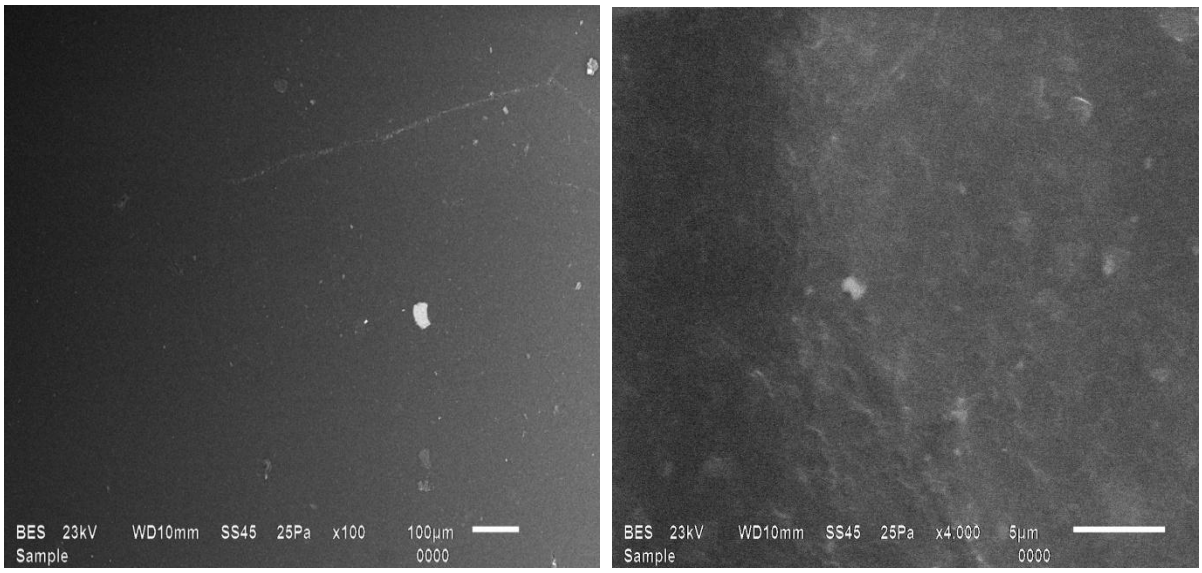

(a) **(b)**

Fig. 5.5 SEM image of nanocomposite having 1wt% clay loading (a) 100x magnification (b) 4000x

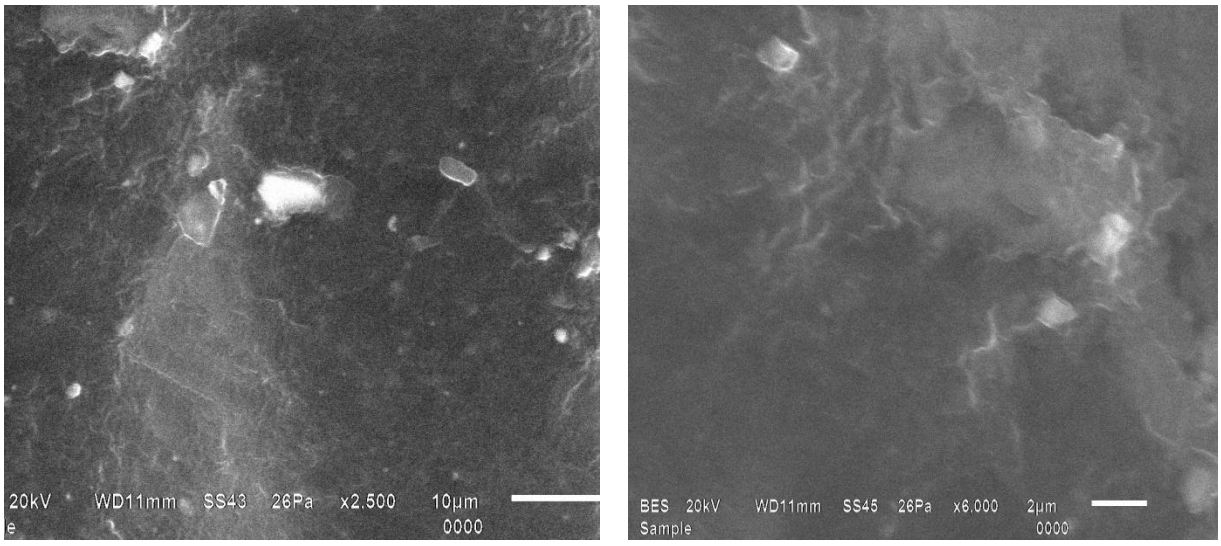

(a) **(b)**

Fig. 5.6 SEM image of nanocomposite having 3wt% clay loading (a) 2500x magnification (b) 6000x

Fig. 5.6 shows SEM image of nanocomposite having 3 wt% of clay loading, in this figure it has been observed that the particles are shown in the matrix are placed some distance apart for one another, which means clay dispersion is good. The image has been again checked at higher magnification and seen that clay particles are dispersed and less particles are visible.

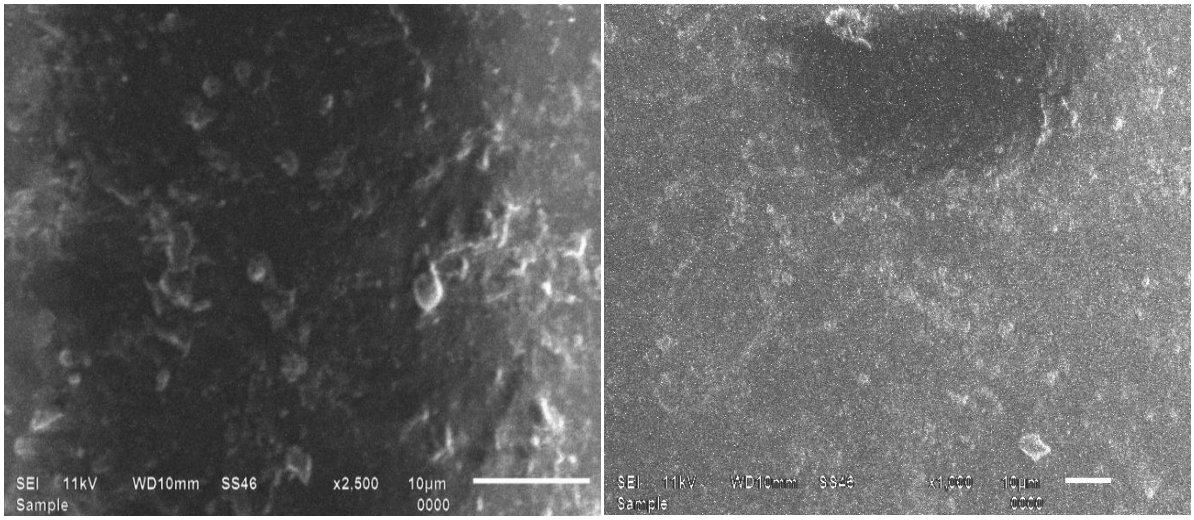

(a) **(b)**

Fig. 5.7 SEM image of nanocomposite having 5wt% clay loading (a) 2500X magnification

(b) 1000x magnification

When the clay loading increases to 5 wt% the dispersion of clay is not proper which is shown by the Fig. 5.7. The cluster of nanoclay clearly seen from this figure, which means the layered silicates are not nano dispersed into the matrix and nanocomposite not formed.

5.2 Macroscopic Behavior

5.2.1 Mode of Failure (Macroscopic Visual Observations)

As per the visual observation the initial specimen had fine shiny epoxy coating and the failure of such specimen under uni-axial tensile load showed an abrupt type and shear type failure. After 15 days of exposure in water baths there was scale formation on all specimen (refer Fig. 5.8). Surface observation showed that epoxy had lost its shine and outer edges on either side showed little fanning out Shear type failure was visible for the initial as well as for 15 days duration specimen (Fig. 5.9).

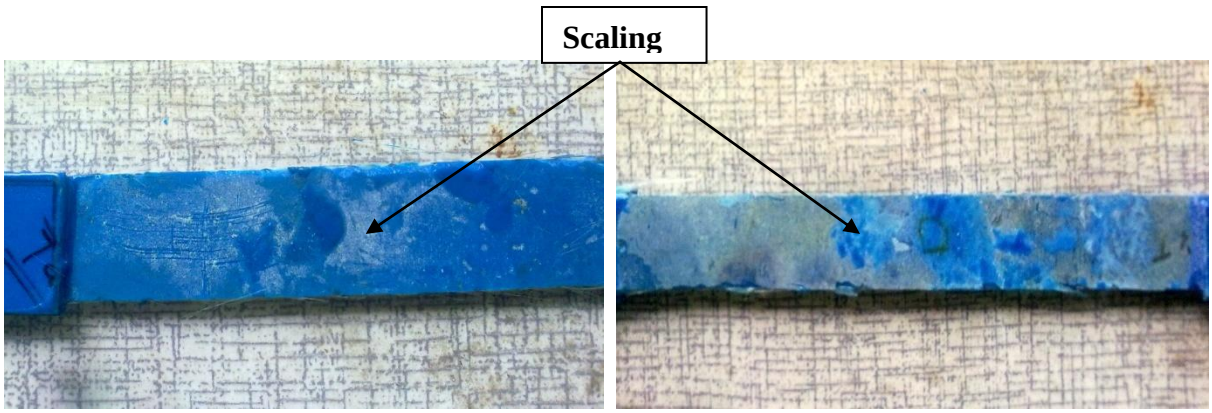

(a) **(b)**

Fig. 5.8 (a) Scaling on sample after 15 days (b) scaling after 30 days

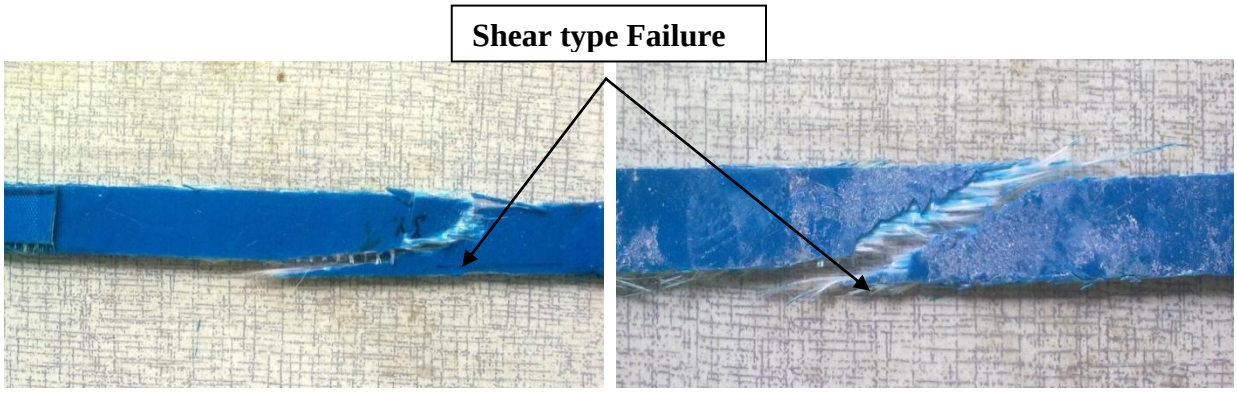

(a) **(b)**

Fig. 5.9 (a) Shear type failure of Water bath samples after 15 days (b) Shear type failure of Water bath samples after 30 day

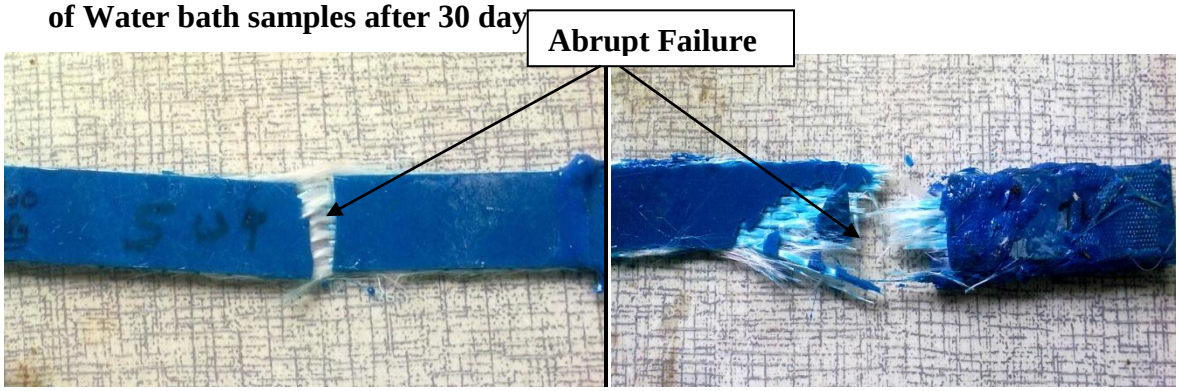

(a) **(b)**

Fig. 5.10 (a) Abrupt failure of NaOH bath samples after 15 days (b) Abrupt failure of NaOH bath samples after 30 days

After 1 months of environmental exposure in water baths observations of degradation and heavy scaling were noted with more scale formation. The NaOH bath samples show more dull surfaces

than simple water and initial samples. Specimens that are immersed in water bath shows shear type failure after 15 days as well as 30 days. The NaOH bath samples show abrupt type failure after 15 as well as 30 days (Fig. 5.10).

5.2.2 Tensile Testing Results of the Samples Simple and Hygrothermally Loaded

Table 5.3 Degradation of Nanocomposite in Water Tank at 45^0C

Water Tank at 45^0C						
No of Days	**Sample Name**	**Sample No**	**Peak load(N)**	**Tensile Strength(MPa)**	**% elongation**	**% Decrease in Strength**
0 Day	0wt%	sample no 1	5200	240	2.6	
		sample no 2	5300	243	2.8	
	1wt%	sample no 1	5500	251	2.1	
		Sample no2	5600	255	2.8	
	3 wt%	Sample no1	5200	300	2.1	
		Sample no2	6400	284	2.2	
	5 wt%	Sample no1	4800	214	1.8	
		Sample no2	6700	299	3.1	
15 Day	0wt%	sample no 1	5200	230	1.6	5.52
		sample no 2	5150	226	1.8	
	1wt%	Sample no1	5300	233	1.4	4.74
		Sample no2	5650	249	1.5	
	3wt%	sample no1	5300	336	1.2	2.39
		Sample no2	5250	234	1.1	
	5wt%	Sample no1	5200	240	1.7	2.14
		Sample no2	6200	262	1.9	
30 Day	0wt%	sample no 1	3370	150	1.1	31.67
		sample no 2	4950	200	1.7	
	1wt%	Sample no1	3700	165	1.6	30.83
		Sample no2	4150	185	1.4	
	3wt%	Sample no1	5050	225	1.7	25.51
		Sample no2	4720	210	1.1	
	5wt%	Sample no1	5800	259	2.3	13.64
		Sample no2	4100	184	1.9	

Table 5.4 Degradation of Nanocomposite in NaOH Tank at 45^0C

NaOH Tank at 45^0C						
No of Days	**Sample Name**	**Sample No**	**Peak load(N)**	**Tensile Strength(MPa)**	**% elongation**	**% Decrease in Strength**
0 Day	0wt%	sample no 1	5200	240	2.6	
		sample no 2	5300	243	2.8	
	1wt%	sample no 1	5500	251	2.1	
		Sample no2	5600	255	2.8	
	3 wt%	Sample no1	5200	300	2.1	
		Sample no2	6400	284	2.2	
	5 wt%	Sample no1	4800	214	1.8	
		Sample no2	6700	299	3.1	
15 Day	0wt%	sample no 1	1740	70.5	1	74.16
		sample no 2	1430	60.3	.7	
	1wt%	Sample no1	1650	77.3	.6	70.82
		Sample no2	1300	63.6	.8	
	3wt%	sample no1	1800	80	.8	73.45
		Sample no2	1700	75	.3	
	5wt%	Sample no1	1700	75.9	.6	71.55
		Sample no2	1575	70	.6	
30 Day	0wt%	sample no 1	660	29.4	0.4	83.95
		sample no 2	1080	48.1	0.9	
	1wt%	Sample no1	1455	64.7	0.6	75.73
		Sample no2	1305	58.1	0.5	
	3wt%	Sample no1	1200	58.4	0.6	82.12
		Sample no2	1000	47	0.9	
	5wt%	Sample no1	1400	64	0.6	75.82
		Sample no2	1200	60	0.6	

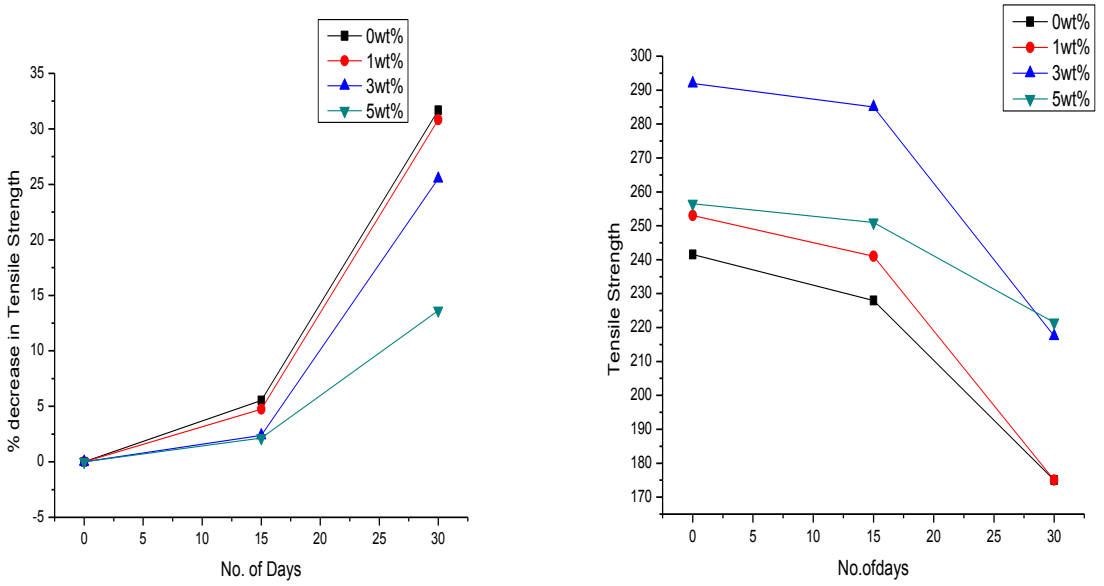

(a) **(b)**

Fig. 5.11 (a) Percent decrease in Tensile Strength (Water bath at 45^{0}C) (b) Tensile Strength degradation (Water bath at 45^{0}C)

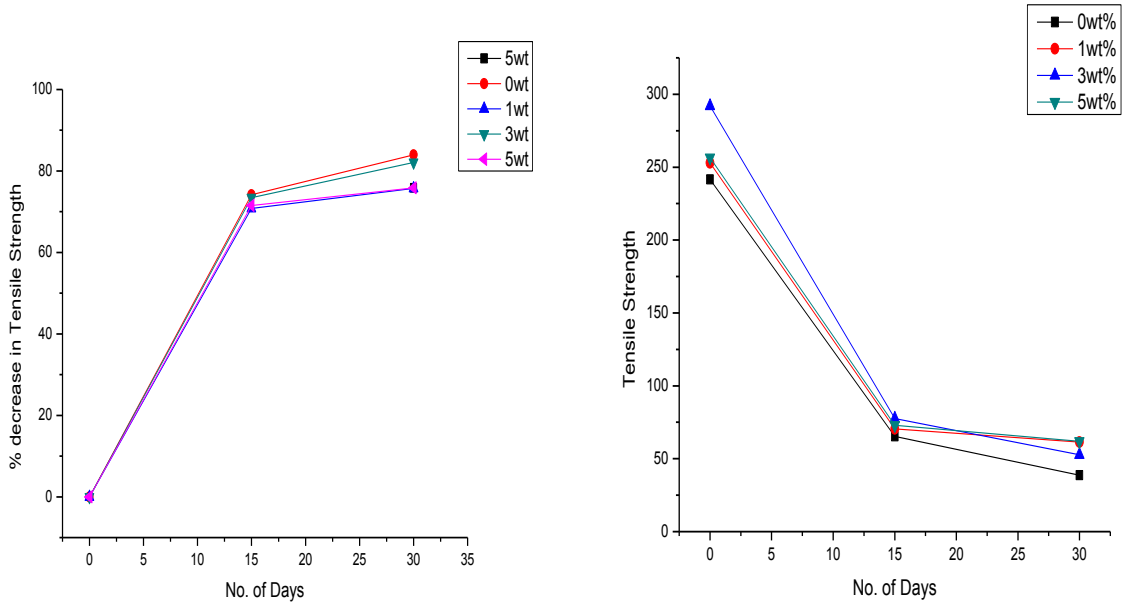

(a) **(b)**

Fig. 5.12 (a) %degradation in Tensile Strength in NaOH bath at 45^{0}C (b) Tensile Strength degradation in NaOH bath at 45^{0}C

From tables 5.3 and 5.4 it is clear that as the clay loading increases the % decrease in strength decreases, which means addition of nanoclay improves the water barrier properties of nano-composites. The tensile strength value of sample having 3 wt% of nanoclay loading is 292 MPa which shows the better tensile properties than other samples. The tensile strength value decreases as the clay loading more than 3 wt percent. After 15 days of water immersion of these samples there is sharp decrease (up to 70%) in tensile strength but in an interval of 15 to 30 days the strength degradation not so much as in first 15 days (10%). It is also seen that the strength degradation in samples immersed in NaOH bath was more severe than samples immersed in simple water.

5.2.3 Bending Test Results of Nanocomposites under Hygrothermal Loading

Table 5.5 Results of Samples for Water Bath at 45^0C

Water Tank at 45^0C						
No of Days	**Sample Name**	**Sample No**	**Peak load (N)**	**Flexural Strength (MPa)**	**Flexural stress at break (MPa)**	**% Decrease in Strength**
0 Day	0wt%	sample no 1	20	59.4	58.2	
		sample no 2	22	67.3	65.1	
	1wt%	sample no 1	22	68	67.5	
		Sample no2	23	72	71.1	
	3 wt%	Sample no1	49	144	143	
		Sample no2	55	160	159.4	
	5 wt%	Sample no1	50	146	144.5	
		Sample no2	57	168	165	
15 Day	0wt%	sample no 1	15.5	45.9	45	13.25
		sample no 2	20	64.3	63.3	
	1wt%	Sample no1	17	50	50	18.57
		Sample no2	20	64	63	
	3wt%	sample no1	52	153	154.8	3.6
		Sample no2	46	140	142	
	5wt%	Sample no1	54	163	161.7	0.6
		Sample no2	44	149	148	

30 Day	0wt%	sample no 1	14.5	43	42	26.59
		sample no 2	17	50	49.3	
	1wt%	Sample no1	18	53	51	24.28
		Sample no2	18	53	52	
	3wt%	Sample no1	40	119	117.3	9.8
		Sample no2	52	155	145	
	5wt%	Sample no1	42	124	114	13.69
		Sample no2	50	147	143	

Table 5.6 Results of Samples from NaOH Bath at 45^0C

NaOH Tank at 45^0C						
No of Days	**Sample Name**	**Sample No.**	**Peak load (N)**	**Flexural Strength (MPa)**	**Flexural stress at break (MPa)**	**% Decrease in Strength**
0 Day	0wt%	sample no 1	20	59.4	58.2	
		sample no 2	22	67.3	65.1	
	1wt%	sample no 1	22	68	67.5	
		Sample no2	23	72	71.1	
	3 wt%	Sample no1	49	144	143	
		Sample no2	55	160	159.4	
	5 wt%	Sample no1	50	146	144.5	
		Sample no2	57	168	165	
15 Day	0wt%	sample no 1	18	53	50	31.88
		sample no 2	12	33.3	30	
	1wt%	Sample no1	19.5	57.5	51	23.92
		Sample no2	16	49	41	
	3wt%	sample no1	50	148	142	8.55
		Sample no2	44.5	131	120	
	5wt%	Sample no1	45	135	123	12.73
		Sample no2	48	140	129	
30 Day	0wt%	sample no 1	13	38	32	32.20
		sample no 2	16	47.9	45	
	1wt%	Sample no1	17	50.4	50.2	24.42
		Sample no2	19	55.4	52	

30 days	3wt%	Sample no1	44	130	112	29.47
		Sample no2	28.5	84.4	81	
	5wt%	Sample no1	33.5	98.6	92.4	28.02
		Sample no2	43.5	129	119	

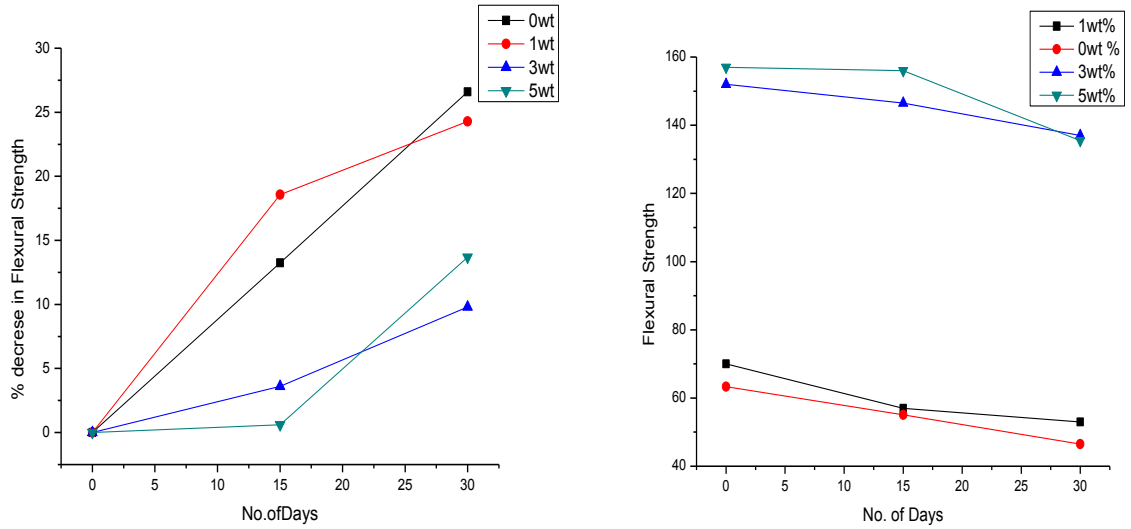

(a) **(b)**

Fig. 5.13 (a) Percent decrease in Flexural Strength (Water bath at 45^{0}C) (b) Flexural Strength degradation (Water bath at 45^{0}C)

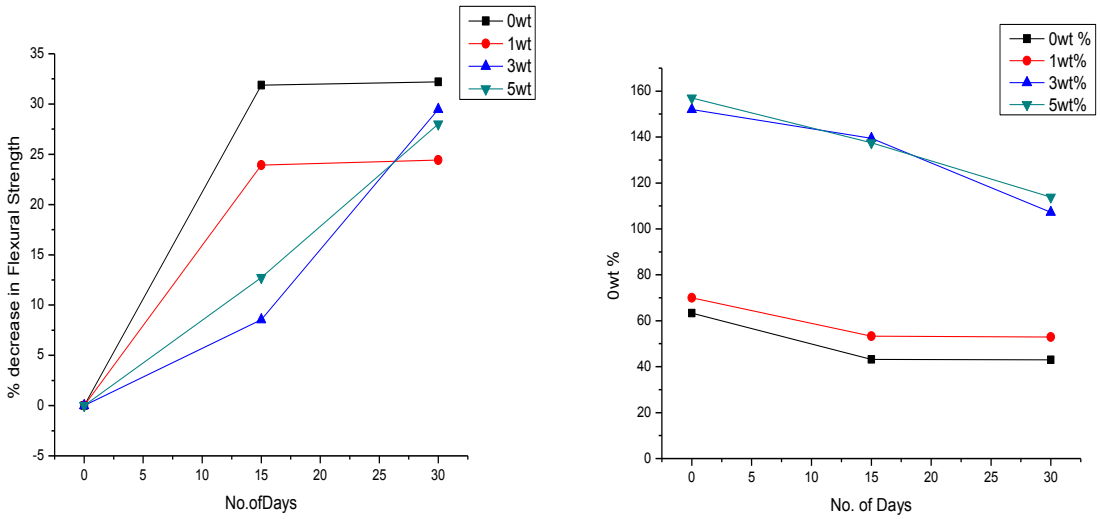

(a) **(b)**

Fig. 5.14 (a) Percent decrease in Flexural Strength (NaOH bath at 45^{0}C) (b) Flexural Strength degradation (NaOH bath at 45^{0}C)

From tables 5.4 and 5.5 it is clear that as the clay loading increases the flexural strength increases. The Flexural strength value of sample having 5 wt% of nanoclay loading is 157 MPa which shows the better flexural properties than other samples. After 15 and 30 days of water immersion, 3 and 5 wt% of nanoclay samples shows better flexural properties than conventional composites. There is a sharp decrease in Flexural strength of conventional composite samples, which means addition of nanoclay improves the water barrier properties of nano-composites.

5.2.4 Rockwell Hardness Test

The Rockwell hardness test is carried out to the different samples, the healthy specimens and the specimens that are undergoing water degradation. The test result values of different samples are shown by the tables below.

Table 5.7 Rockwell Hardness Values for Healthy (without water degradation) Samples

Clay loading → / loading points ↓	Rockwell Hardness Values			
	0 wt%	**1 wt%**	**3 wt%**	**5 wt%**
Point 1	33	38	42	32
Point 2	33	31	34	31
Point 3	34	32	40	31
Point 4	33	34	35	32
Point 5	35	39	36	33
Average	**33.3**	**34.7**	**37**	**31.7**

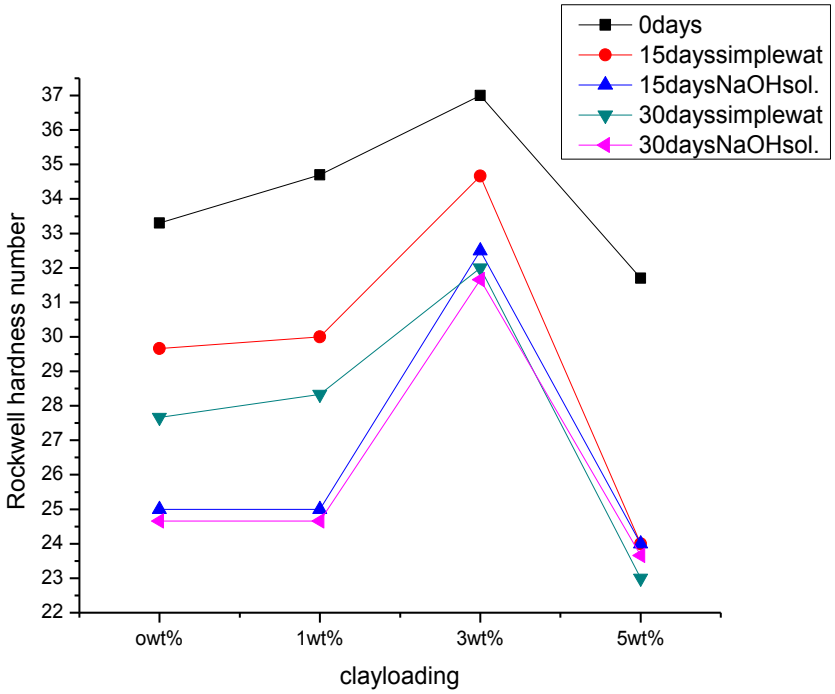

Fig. 5.15 Rockwell hardness values graph for different samples

Table 5.8 Rockwell Hardness Values of Samples Undergoing Water Immersion

No. of days under water	loading points	Rockwell Hardness Values			
		0 wt%	1 wt%	3 wt%	5 wt%
15 days Simple water	P1	30	32	29	20
	P2	27	33	35	23
	P3	31	28	32	22
	P4	29	30	37	26
	P5	30	25	40	24
	AVG.	**29.66**	**30**	**34.66**	**24**
15 days NaOH water	P1	25	25	32	25
	P2	28	24	29	27
	P3	21	23	33	21
	P4	24	24	32	20
	P5	25	26	34	28
	AVG.	**25**	**25**	**32.5**	**24**

30 days Simple water	**P1**	30	30	28	23
	P2	29	26	33	23
	P3	27	30	35	22
	P4	26	28	35	24
	P5	27	27	28	23
	AVG.	**27.66**	**28.33**	**32**	**23**
30 days NaOH water	**P1**	26	25	30	22
	P2	23	25	32	23
	P3	25	23	33	26
	P4	23	24	32	27
	P5	29	31	31	21
	AVG.	**24.66**	**24.66**	**31.66**	**23.66**

This test has been performed to check the effect of water on the matrix of nanocomposite. Fig.5.15 shows that when samples have been dipped into the different water baths the hardness decreases day by day. It has been clearly seen that simple water at 45^0C had less effect on the hardness of the matrix as compared to water having some wt% of NaOH into it. As the day increases the hardness decreases. It has been also seen that as the clay loading increases to 0 to 3 wt% the hardness values increases. But after more clay addition hardness get decreases. This is due to the exfoliation of the clay particles into the matrix which reduced the intake capacity of water into the matrix. Nanocomposites containing 3 wt% of clay shows the best results among all other samples. This can also indicates that at 3 wt% exfoliation was achieved as discussed in the microscopic behavior of these nanocomposites.

CHAPTER 6 CONCLUSION AND FUTURE SCOPE

6.1 Conclusion

Fiber reinforced nanocomposites have been manufactured using glass fiber as reinforcement and epoxy mixed with Closite 30 B as matrix. Nanoclay was added to epoxy in different weight percentage (1 wt%, 3 wt% and 5 wt% of weight of resin). For the processing of epoxy-nanoclay mechanical stirring and ultrasonication was done. The composites were manufactured using hand layup method and characterized using SEM and XRD. Better intercalation of clay in epoxy was observed in samples with 1 and 3 wt% clay loadings. Clay agglomerates were found in 5 wt% samples. Tensile and bending tests were performed on nanocomposites as per ASTM standards. It was found that the hardness of the nanocomposites increased with increasing nanoclay content. However, it was also seen that there was an optimal limit. Tensile strength and flexural strength of the 3 wt% and 5 wt% clay content samples were improved. The durability studies were conducted on nanocomposites by exposing to water and alkaline medium for a period of one month then evaluating the mechanical property degradations. Mechanical properties were found to degrade with increase in time. 3 wt% GFRP composites showed less degradation and better properties under all conditions over neat counterparts. The water resistance property of epoxy was improved by the addition of both glass fibre and nanoclay, which is maybe attributed to the increasing of the tortuosity path for water penetration.

6.2 Future Scope

1. To see the effect of nanofillers on FRP`s, experiments can be repeated by changing the type of nanofillers.
2. The experiment can be performed on polyester as matrix system, since with this matrix the barrier properties of composites can be enhanced.
3. Clay loading can also be varied more than 5 wt%.
4. The duration of current experiment can be increased to see the effect in long term.
5. The strength of alkaline aqueous solution can be varied to see the change in chemical attack.

REFERENCES

www.whitebuffalobeadsandstones.com & www.ia.ucsb.edu

www.wikipedia.com/Composite material.html

w**w**w.structsource.com/pdf/composite.pdf

www.emba.uvm.edu/iatridis/me257/Introduction.html

www.engr.sjsu.edu/sgleixner/PRIME/FRP.pdf

www.autospeed.com/composites.html

Alexandre M, (2000), Polymer-layered Silicate Nanocomposites: Preparation, Properties and uses of a New Class of Materials. Mater. Sci. Eng. Rep., 28, 1-63.

Avila A, Horacio V. and Marcelo I. (2005), The nanoclay influence on impact response of laminated plates. Latin American journal of solids and structures, 3, 3-20.

Avila A, Almir S and Marcelo I. (2006), A study on nanostructured plates behavior under low-velocity impact loading. Material and design, 34, 28-41.

"Bragg's Law," http://hyperphysics.phyastr.gsu.edu/hbase/quantum/bragg.html, 2006.

Berketis K, Tzetzis D and Hogg P.J, (2007), The influence of long term water immersion ageing on impact damage behaviour and residual compression strength of glass fibre reinforced polymer (GFRP). Material and design, 29, 1300-1310.

Biron, M. (1973), Thermosets and Composites-Technical Information for Plastics Users. New York: Elsevier.

Chow W, Bakar A and Ishak Mohamad A , (2005), Water absorption and hygrothermal aging study on organomontomorrillonite reinforced polyamide6/polypropylene nanocomposites. Journal of applied polymer science, vol 98, 780-790.

Chun-Ki Lam, Hoi-yan and Kin-tak Lau (2004), Cluster size effect in hardness of nanoclay/epoxy composites. Composites, vol 36 , 263–269.

Gao Shang-Lin, Mader E and Plonka R., (2007), Nanocomposite coating for healing surface defects of glass fiber and improving interfacial adhesion. Composite science and technology, 68, 2892-2901.

Isil Isik, Ulku Yilmazer and Goknur Bayram (2003), Impact modified epoxy/montmorillonite nanocomposites: synthesis and characterization. Polymer, 44, 6371–6377.

Jena P, (1996), Nanostructured materials**.** Nova Science New York 1996.

Kornmann X, Rees M, Thomsan Y, Necola A, Barbezat M and Thomsan R, (2005), Epoxy layered silicate nanocomposite as matrix in glass fiber-reinforced composites. Composite science and technology, 65, 2259-2268.

Lei Wang, Ke Wang, Ling Chen and Chaobin He, (2006), Hygrothermal Effects on the Thermo-mechanical Properties of High Performance Epoxy/Clay Nanocomposites. Polymer engineering science, 46, 215–221.

Lowenstein, K. L. (1973), Manufacturing Technology of Continuous Glass Fibers. New York: Elsevier.

Manjunatha C.M, Taylor A.C, Kinloch A.J and Sprenger S, (2009), The tensile fatigue behavior of a silica nanoparticle-modified glass fiber reinforced epoxy composites. Composite science and technology, 70, 193-199.

Nanostructured and quantum effects (H Sakaki and H. Noge, eds) Springer Verlag, Berlin (1994).

Njuguna J and Pielichowski K, *Advanced Engineering Materials*, 5, 769 (2003).

Quaresimin M. and Varley R. J, (2007), Understanding the effect of nano-modifier addition upon the properties of fibre reinforced laminates. Composite science and technology, 68, 718-726.

Sinha R. S., Okamoto M., (2003), Polymer/layered silicate nanocomposites: a review from preparation to processing. Prog. Polym. Sci., 28, 1539–1641.

Wang H, Zeng C, Elkovitch M and Koelling W. K, (2001), Processing and properties of polymeric nanocomposites. Polymer engineering and science, 41, 11.

Wetzel B, Rosso P, Haupert F and Friedrich K, (2006), Epoxy nanocomposite-fracture and toughening mechanisms. Engineering fracture mechanics, 73, 2375-2398.

Yasmin A, Luo J.J, Abot J.L, Danial I.M, (2006), Mechanical and thermal behavior of clay/epoxy nanocomposites. Composite science and technology, 66, 2415-2422.

Zainuddin S, Hosur M.V, Zhou Y, Kumar Ashok and Jeelani S, (2010), Durability study of neat/nanophased GFRP composite subjected to different environmental conditioning. Material science and engineering, A 57, 3091-3099.